

## CHAPTER 4: DC/RF INJECTORS

BRUCE M. DUNHAM

*Department of Physics and CLASSE*

*Wilson Laboratory*

*Cornell University*

*Ithaca, NY 14853*

### Keywords

DC Electron Gun, High Voltage, Photocathode, Low Emittance, Photoemission, Superconducting RF, Laser, Laser Shaping, High Power, High Brightness

### Abstract

A high voltage DC photoemission electron gun followed by an RF accelerating module is presently the best solution for generating high average power electron beams of moderate bunch charge, particularly for energy recovery linac based light sources and for free-electron lasers. Most modern injectors for accelerators use a photocathode illuminated by a pulsed laser which is synchronized to the RF system. This allows one to produce a variety of bunch trains that can be tailored to the needs of a particular machine by modulating the laser appropriately. High gun voltages, above 300 kV, are required in order to combat the emittance growth due to space charge in tightly bunched beams. The emittance growth varies greatly depending on the exact electron bunch dimensions, but DC guns are most often used for bunch charges up to a few hundred picocoulombs. High average beam powers are possible using a DC gun as most of the energy can be directly coupled into the beam, with very little lost in wall heating as is the case for normal conducting RF guns. The gun itself is followed by an emittance compensation section and a high average power RF accelerating section, often superconducting. This chapter will cover the history of DC gun based injectors, system level and sub-system level requirements and the practical details needed to design and construct a device.

## 4.1 INTRODUCTION

One of the first accelerator applications of DC photoemission guns was a GaAs polarized electron source at the SLAC [4.1]. This source used a relatively low voltage gun (~100 kV) followed by a standard RF bunching and accelerating section [4.2]. Chapter 8 details the design of a polarized source. Over time, these morphed into higher voltage, unpolarized DC photoemission sources that directly provided bunched beams, eliminating much of the complexity of RF manipulation associated with chopping a DC or quasi-DC beam to produce a bunch train. This chapter covers the design and implementation of an electron injector using such high voltage DC photoemission guns and an RF accelerator.

There are two main benefits of increasing the gun voltage well above 100 kV. For low bunch charges or quasi-DC beams 100 kV is adequate, but as the bunch charge increases, space charge forces become important and higher voltages are needed to reduce their promotion of emittance growth. The second benefit is that for a high enough voltage (say greater than 250 kV), a pre-acceleration cavity (often called a capture section) is not required, which shrinks the size and complexity of the injector. The RF guns discussed in other chapters also have these benefits.

The Lasertron was one of the first higher voltage DC photoemission guns [4.3]. This was a scaled-up version of a SLAC polarized source, operating at ~400 kV, and applicable as a driver for an RF power source. A similar device, designed and constructed as a high average power electron source for an FEL at Jefferson Lab [4.4], has operated at up to 9 mA and 350 kV for many years.

Problems with HV breakdown were common in early guns (and still are), as the cathodes (GaAs) were activated in the gun's vacuum chamber using cesium to generate high quantum efficiencies. Cesium contamination makes breakdown more likely, as it lowers the work function of the high voltage electrodes. To overcome this problem and make it easier to change cathodes without breaking vacuum, cathode load-lock systems (common in semiconductor industries) were introduced [4.5] so that the cathodes could be prepared in a separate vacuum chamber. The first systems were difficult to use as the load-lock hardware was attached to the gun's high voltage end, making changing and activating cathodes a slow process. In newer guns [4.6], the system's geometry was changed to allow the load-lock to be at ground potential, considerably simplifying the design and operation of that process. Today, one can swap cathodes in a matter of minutes, minimizing downtime and eliminating the HV problems caused by cesium.

Many currently operational DC photoemission guns use a scaled-up version of the original SLAC polarized source. They all continue to suffer from high voltage problems and several laboratories are devising new HV designs to overcome these deficiencies, which are described later in this chapter. Considerable work has been done on electron guns with pulsed high voltage [4.7], but much of this is not directly applicable to DC photoemission guns so will not be covered.

Over time, RF guns (see Chapters 1, 2 and 3) have become very popular due to their ability to produce high bunch charges and high beam energy with good emittance in a relatively small footprint. Recent detailed optimization studies [4.8] of DC photoemission guns followed by RF accelerating sections showing excellent results have renewed interest in this scheme, prompting many laboratories to pursue variants of the basic DC gun design. These studies revealed that it is possible to nearly re-capture the initial thermal emittance of the electron beam generated at the cathode after acceleration to many mega electron volts. DC guns also allow the use of GaAs-like cathodes that have the lowest thermal emittance of any current cathodes [4.9], thus providing a path for extremely bright electron-beam injectors. The other advantage of DC guns/RF injectors is that high average powers are relatively straightforward to obtain, with designs up to 100 mA of average current at 5-10 MeV being tested. In some instances, RF guns can produce high average powers [4.10].

In the next section, we will look at the parameters and requirements for electron injectors and demonstrate that the choice of injector depends on the desired operational goals.

## 4.2 SYSTEM-LEVEL REQUIREMENTS AND DEFINITIONS

The needs of the main accelerator, and ultimately the experiment's beam, will be used for determining the requirements for the electron injector. So, a common question is what type of electron injector is most appropriate to use from the types described in this book? Table 4.1 lists the important parameters.

For example, systems requiring high bunch charge ( $> 1$  nC) and low average power will be best served by an RF gun. System needing a lower bunch charge (less than a few hundred picocoulombs) and high average current ( $> 1$  mA) often will use a DC type gun, while superconducting (SC) RF guns fill the gap between NCRF- and DC-guns. If polarized beams are needed, then only DC guns are appropriate, which will limit some other choices of parameters.

For the rest of this chapter, I discuss only the DC gun/RF injector, within the parameter ranges in Table 4.2. If polarized electrons are required, one must use GaAs-like photocathodes that have a very special list of additional requirements, covered in detail in Chapter 8. GaAs has several other special attributes that make

it desirable even for non-polarized beams; in the rest of this chapter, I will assume semiconductor cathodes are used.

Parameter	Min	Max
Polarized Beam?		
Bunch Charge [pC]	$10^{-3}$	$10^4$
Average Current [mA]	$10^{-3}$	$10^2$
Duty Factor [%]	~0	100
Emittance [mm mrad rms, normalized]	0.1	> 10
Final Beam Energy [MeV]	0.5	20
Bunch Length [Degree of RF phase]	0.1	10
RF Frequency [MHz]	100	3 000

Table 4.1. Important parameters for electron injectors, with typical minimum- and maximum-values of interest.

Parameter	Range
Polarized Beam?	No
Bunch Charge	0-200 pC
Average Current	0-100 mA
Duty Factor	0-100%
Emittance	< 2 mm mrad rms normalized
Final Beam Energy	5-15 MeV
Bunch Length	< 1 deg
Frequency	1 300 MHz

Table 4.2. Range of parameters used for the discussions in this section.

Before continuing, several terms and definitions need to be covered. An important concept is the difference between continuous wave (CW), DC and pulsed, when applied to high voltage and beams. DC means that the high voltage power supply is always on and connected across the gun's cathode-anode gap, or that the electron beam is always on. Pulsed signifies that the power supply is only on for a brief period, overlapping the time when the electron beam is extracted from the cathode. Many industrial devices are pulsed (*e.g.*, X-ray tubes, klystrons, modulators). For such systems, pulse durations are typically less than 1  $\mu$ s, and pulsed power operators consider anything longer than that to be DC. For this chapter, DC means "always on". CW denotes that for each period of an RF cycle, a bunch of electrons is present. The DC/RF photoemission injectors discussed here are a hybrid system, since the gun voltage is always on (DC) and a laser generates electrons to fill each RF period (CW). The RF guns discussed in Chapter 3 typically are pulsed-mode devices, but CW versions can be built.

Other important concepts are the thermal emittance and beam brightness. Assuming that the emitted electrons follow a Maxwellian transverse velocity distribution, the transverse-momentum spread of the electrons is  $\sigma_{p,rms} = \sqrt{mkT}$ , where  $kT$  is the electrons' effective transverse energy and  $m$  is the mass of the

electron. For a negative electron affinity cathode (NEA) like GaAs, illuminated with a wavelength near the band gap,  $kT$  approaches the temperature of the crystal (at room temperature,  $kT = 25$  meV where  $k$  is the Boltzmann constant and  $T$  is the temperature). For non-NEA cathodes,  $kT$  will be above the cathode temperature, and if GaAs is illuminated with a wavelength greater than the band gap, the effective temperature also will increase. Knowing  $kT_{\perp}$ , the normalized, transverse thermal-emittance of a beam from a photocathode,  $\epsilon_{n,rms,th}$ , is calculated from [4.11]

$$\epsilon_{n,rms,th} = \sigma_{laser,rms} \sqrt{\frac{kT_{\perp}}{mc^2}} \quad (4.1)$$

where  $\sigma_{laser,rms}$  is the rms laser spot size at the cathode and  $c$  is the speed of light in a vacuum. This holds only when the charge per bunch is low enough that space charge forces are not a concern. Thus, finding cathodes with the smallest  $kT$  is crucial for low emittance guns.

For a given electric field at the cathode surface,  $E_{cathode}$ , Gauss' Law gives the maximum emission charge density,  $\sigma$ , that can be supported for a pancake beam,  $\sigma = E_{cathode} \epsilon_0$ , where  $\epsilon_0$  is the permeability of free space. If a charge per bunch  $q$  is required, then the area of the laser beam must be greater than or equal to  $q \sigma^{-1}$  for a uniform laser distribution. This sets a minimum value on the thermal emittance, as the laser area (and spot size,  $\sigma_{laser}$ ) is then determined from  $E_{cathode}$  for the desired charge per bunch. This is a reason to push the electric field at the cathode as high as possible. Doubling the field allows the laser radius to be reduced by  $\sqrt{2}$  for a constant charge, subsequently reducing the emittance by  $\sqrt{2}$ .

The brightness of the electron beam is another important term to understand, as the X-ray beam brightness produced by a light source (storage ring or Energy Recovery Linac) is related directly to it. The transverse, normalized beam brightness,  $B_n$ , is defined as

$$B_n = \frac{2I}{\pi^2 \epsilon_{(n,x)} \epsilon_{(n,y)}} \quad (4.2)$$

where  $I$  is the beam current, and  $\epsilon_{(n,x)}$  and  $\epsilon_{(n,y)}$  are the normalized emittances in the transverse planes. The maximum transverse brightness for an electron bunch was recently shown to be given by [4.11]

$$\frac{B_n}{f} = \frac{mc^2 \epsilon_0 E_{cathode}}{2\pi kT} \quad (4.3)$$

where  $f$  is the repetition frequency of the bunch train. The importance of this equation is that the maximum obtainable beam brightness depends not on the actual bunch charge, but solely on the transverse thermal energy of the emitted electrons and the electric field at the cathode surface at the time of emission. This again demonstrates the drive to increase the field at the cathode and to identify cathodes with the lowest possible  $kT$ .

Figure 4.1 is a block diagram of a DC/RF photoinjector. To control the space charge forces, the initial bunch length exiting the gun is set to  $\sim 30$ -40 ps (for 1 300 MHz) due to the relatively low initial beam energy (compared to an RF gun). The bunch is compressed further as it passes through an RF buncher cavity (normal conducting (NC) in this case) to 5-10 ps at the entrance to the accelerating cavities. The beam then

is compressed even more and accelerated as it passes through several SCRF cavities, to a final bunch length of 1-2 ps. The solenoidal focusing magnets control the beam size and compensate for emittance [4.12].

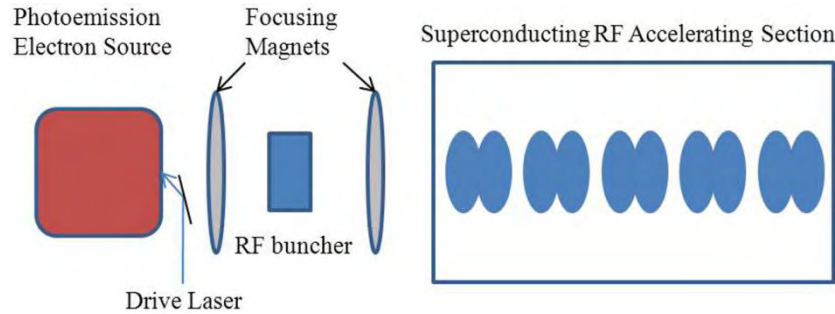


Figure 4.1. Schematic of a typical electron injector using a DC photoemission gun and a superconducting RF accelerator section.

For comparison, Figure 4.2 illustrates a thermionic electron gun-based injector [4.5]. In this arrangement the output beam is either DC or has a long pulse (for a gridded gun). To reduce the bunch length enough for injection into RF accelerating cavities, several extra steps are required. In some instances, a chopper system “chops” out a fraction of the beam in time, so that the bunches are at the proper repetition frequency (or sub-harmonic thereof). Then, one or more sub-harmonic- or harmonic-buncher cavities compress the bunches further until they are ready for acceleration. If the gun’s voltage is too low, a pre-acceleration cavity may be necessary to boost the energy high enough for injection into the final set of accelerating cavities. Solenoid magnets along part or all of the beamline provide focusing. These systems have been used successfully for many years, but are more complex, less efficient and cannot provide the beam quality needed for some of today’s demanding applications.

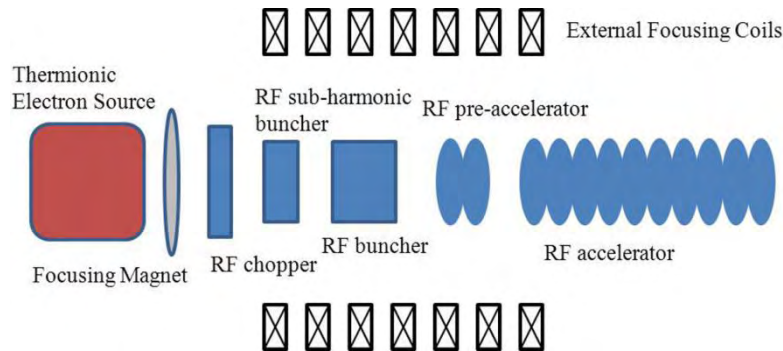


Figure 4.2. A typical set-up for an electron injector using a thermionic gun and a complicated RF section for chopping, bunching and acceleration.

## 4.3 SUB-SYSTEM DESCRIPTION

### 4.3.1 Overview

Designing and constructing the components of a DC photoemission electron-source-based, high average power injector is a difficult task: it still is evolving as more and more laboratories become involved. In this section, I describe the design and construction of the sub-systems of a DC photoemission gun/RF injector

### 4.3.2 High Voltage Gun

Simulations [4.8] show that, up to a certain point, a higher gun voltage is important for obtaining low emittance, after which the improvement is relatively small. Thus, a DC gun operating between 400-600 kV with the appropriate cathode should meet the emittance goals (Table 4.2) for many high performance applications.

To operate in this range, the gun must be processed to 10-25% above the operating value to reduce field emission and arcing; consequently, a 600 kV operational voltage requires a gun designed to withstand 750 kV maximum voltage. Figure 4.3 is a schematic cutaway of a DC photoemission gun, designed to meet the requirements in Table 4.2. This particular gun was operated for over a year using a test beamline to measure the performance of the gun and cathode before it was incorporated into the rest of the injector. Details of these measurements were published elsewhere [4.13]; the main result was that the emittance measurements at 77 pC per bunch and 250 kV beam energy match the simulations very closely, giving confidence that the latter are accurate.

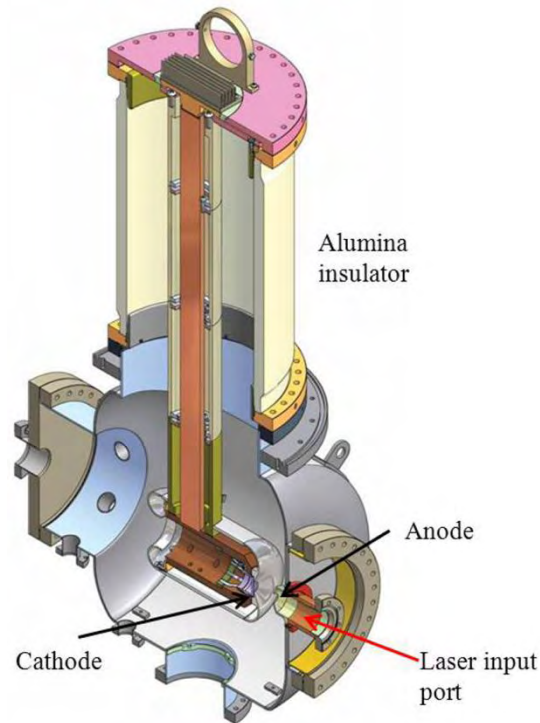


Figure 4.3. A cutaway view of a DC photoemission gun. [Adapted with permission from [4.14]. Copyright 2008, American Institute of Physics]

Sections 4.3.2.1 through 4.3.2.6 describe the gun's components.

#### 4.3.2.1 Photocathode Materials

A perfect photocathode for an accelerator electron source would have high efficiency at a convenient laser wavelength, a fast response time, a long lifetime and a low thermal emittance. Unfortunately, no such cathode exists, although the search continues. Several different photocathodes meet some of these criteria, so tradeoffs must be made depending on a particular system's requirements. For an ERL application, obtaining 100 mA average current necessitates having high quantum efficiency (QE) photocathodes.

Currently, semiconductor photocathodes are the best choice for high QE and low emittance. Examples are GaAs, Cs<sub>2</sub>Te, GaN and K<sub>2</sub>CsSb. Both Cs<sub>2</sub>Te [4.15] and GaN [4.16] show promise, but require UV light; no laser systems yet can produce enough average power in the UV spectrum for 100 mA operation. Both GaAs and K<sub>2</sub>CsSb have 5-10% QE for ~520 nm light, where high average power lasers are readily available. In this chapter, only semiconductor cathodes are covered; Chapters 6, Chapter 7 and Chapter 8 discuss other types of cathodes for photoemission guns.

As mentioned earlier, nearly all the intrinsic thermal emittance from the cathode is recoverable using a carefully designed emittance compensation scheme. Of all the cathodes available, GaAs has the lowest thermal emittance [4.9], and is thus the one of choice for ultimate brightness. Unfortunately, the QE is near a minimum when the thermal emittance is smallest (close to the band gap), thus, it is unsuitable for high average current, so a compromise must be made between QE and emittance. Figure 4.4 demonstrates that the transverse electron energy at 520 nm is approximately 4X larger than at the band gap wavelength (850 nm). Quantum efficiencies of 5-20% can be reached at 520 nm, but fall quickly to less than 1% as the band gap wavelength is approached.

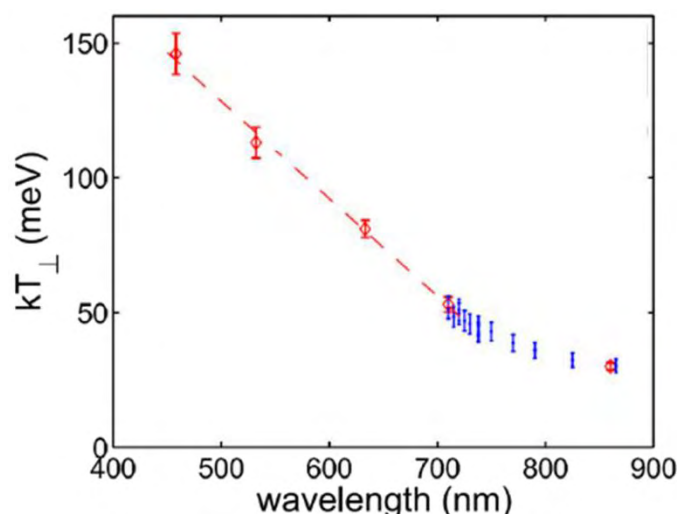


Figure 4.4. Transverse thermal energy for the electrons photoemitted from GaAs as a function of wavelength [4.13]. The red points were measured using multiple laser spot sizes while the blue points were measured using a single spot size. The dashed line shows a fit over the linear region.  $kT_{\perp}$  is the electron's effective transverse energy normal to the cathode's surface. [Reprinted with permission from [4.13]. Copyright 2008, American Institute of Physics.]

In addition, it is known that at  $\sim 780$  nm a fast laser pulse will generate an electron beam with a  $\sim 10$  ps long tail [4.17], which is unacceptable for low emittance operation. For shorter wavelengths ( $\sim 520$  nm), recent measurements [4.13] show (Table 4.3) that the response time is quite fast ( $\sim 1$  ps) provided that the QE is not too high ( $< 10\%$ ); this phenomenon is related to the absorption depth of light versus wavelength. Near the band gap, GaAs is nearly transparent, and thus, the electrons are produced deep in the material and take longer to reach the surface. The longer extraction time, though, gives the electrons more time to thermalize into the conduction band minimum, reducing their effective temperature. This example highlights some of the tradeoffs that must be made even when using GaAs; an operating wavelength of  $\sim 520$  nm often is chosen as the best compromise between QE, thermal emittance, response time and available lasers. Some people have suggested using sufficiently thin layers of GaAs to overcome this problem, thin enough that the electron's transit time is shorter than that due to the absorption depth [4.18]. These layered cathodes, grown on glass and used in transmission mode, may simplify delivery of the laser to the cathode.

Wavelength [nm]	$\tau$ at 250 kV [ps]
860	$69 \pm 22$
785	$9.3 \pm 1.1$
710	$5.2 \pm 0.5$
520	$< 1.0$
460	$< 0.14$

Table 4.3. GaAs response time,  $\tau$ , for various laser wavelengths [4.13].

While GaAs offers the very high quantum efficiencies necessary for high power guns, it also is prone to generating a “halo” from unintended areas of the cathode. The cathode’s surface is usually larger than the size of the electron beam (and the laser spot) to assure a uniform electric field across the emission area. Any stray or scattered light hitting outside the desired spot generates accidental electrons (Figure 4.5). This drawback turned out to be the biggest factor in the poor cathode lifetime in the Jefferson Laboratory’s polarized source [4.19]. Electrons generated near the edge of the electrode from stray light experienced non-uniform fields and eventually hit the vacuum chamber walls, producing secondaries, X-rays, UV light and increasing the vacuum, which all degrade the cathode’s longevity.

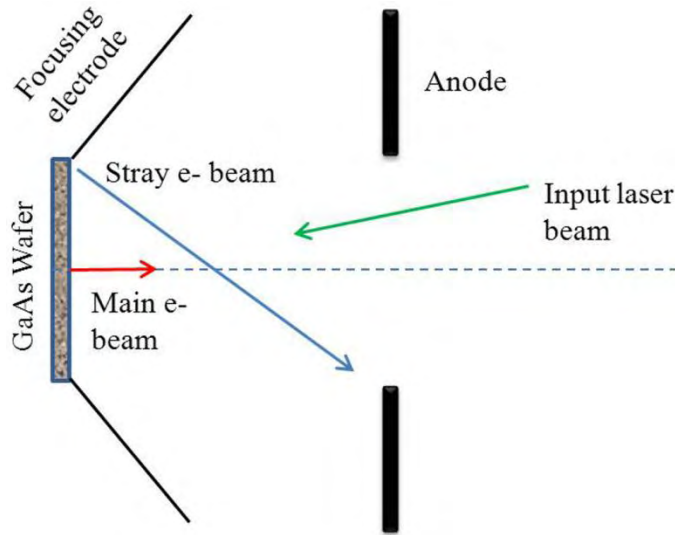


Figure 4.5. Stray light can hit any part of the cathode’s surface, thereby producing electrons. Electrons generated in non-uniform field regions (blue) can be deflected to hit the vacuum chamber walls.

To overcome this problem, the outer area of the cathode must be inactive so it cannot emit electrons. One way to accomplish this is to cover the wafer with an oxide layer (deposited in an electrochemical cell using a weak solution of phosphoric acid) and then strip off the oxide at the center of the wafer (Figure 4.6). Another way is to mask the wafer when depositing the cesium during activation.

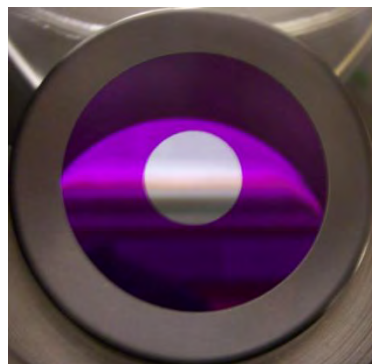
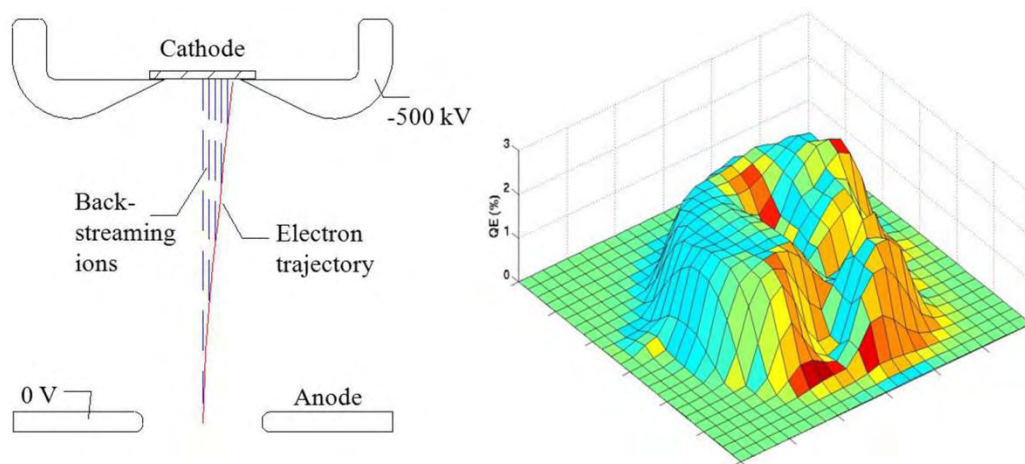


Figure 4.6. The central silver circle is the active area of the GaAs cathode, while the purple area was anodized to inhibit electron emission. A tantalum retaining ring (gray) surrounds the wafer.

The last important parameter is cathode lifetime. The cathodes described above are all somewhat sensitive to chemical poisoning, requiring an ultra-high vacuum (UHV) environment. GaAs is the most sensitive, unfortunately requiring vacuum levels  $< 1 \times 10^{-9}$  Pa to operate successfully. An additional lifetime limiter is ion back-bombardment that further lowers the QE. The electron beam can ionize residual gas molecules

anywhere along their path, which then can be accelerated back towards the cathode's surface. Jefferson Laboratory's researchers [4.20] carried out extensive measurements at 10 mA average current and measured cathode lifetimes as high as  $10^6$  C cm<sup>-2</sup> (the amount of charge extracted per square-centimeter when the QE has fallen by  $1/e$ ). We can use this data to estimate that a 10 W maximum power laser system should provide 100 mA over 100 hr with a 1.8 mm diameter laser spot [4.21]. Such performance in an operational environment has not been demonstrated; certainly, it is an optimistic estimate.

Figure 4.7 illustrates what happens during ion back-bombardment. An electron (red trajectory) is accelerated and can ionize any gas in its path. The ions (blue trajectories) are then accelerated back towards the cathode in a straight line due to their larger mass. The maximum in the ionization cross section is in the 50-100 V range, so many ions are created close to the cathode's surface, but also can be produced, with lower probability, anywhere between the cathode and anode, and beyond the anode. The right part of the figure shows an actual quantum efficiency map of a cathode after operating with the laser positioned off-center. The ion damage at the laser spot and a trough between it and the center of the cathode is clearly visible. The most straightforward method for reducing ion back-bombardment for GaAs is to lower the partial pressure of the background gas species as much as possible.



**Figure 4.7.** Electrons leaving the cathode (red) ionize residual gases that then are accelerated back to the cathode (blue). The QE map on the right is from a cathode undergoing ion back-bombardment (arbitrary color map). The laser was positioned off-center, and the ions produced a channel from the laser's position to the electrical center of the cathode. [Adapted with permission from [4.22]. Copyright 1, American Institute of Physics]

Many groups worldwide continue to investigate new cathode materials for electron sources and detectors. Reference [4.23] gives a good summary of recent work.

#### 4.3.2.2 Load-Lock System

The semiconductor industry has used load-lock systems for many years to introduce wafers into the processing system without having to open the entire vacuum system. Similar reasons drove the development of load-lock systems for photoemission guns, and now they are a standard component for most new guns.

As part of GaAs activation, the cathode material is heat-cleaned to remove surface contaminants and then activated with cesium and an oxidant. For all the early photoguns, this was done inside the gun vacuum chamber [4.24]. However, this is detrimental to high voltage performance for two reasons. First, heating the cathode also heats high voltage surfaces that previously were conditioned; this can alter the electrode surfaces enough to degrade the voltage hold-off strength. Second, the cesium added to the cathode can end up on the high voltage surfaces, locally reducing their work function and increasing the probability of field

emission. In addition, installing a new cathode meant breaking the vacuum and re-baking, a 1-2 week process, which is incompatible with accelerator operations.

While a number of designs were tried for keeping the cesium from reaching the electrodes, the only sure way is to separate the functions of preparing the cathode from the gun, and to use a load-lock system. The Stanford Linear Collider polarized source [4.25] tried several load-lock configurations to improve the gun's reliability. In one, the load-lock hardware was on the gun's high voltage end, requiring a large high voltage enclosure and limited access to when the gun was turned off. Now, several guns have altered the system geometry to allow the load-lock to be at ground potential, simplifying the design and operability (Figure 4.3).

Below is a list of typical requirements for a photocathode load-lock system. Some of the functions may be combined in a single chamber, if desired. The functions may vary depending on the cathode type.

- separate chamber for loading new cathodes, including quick bake-out capabilities
- cathode cleaning chamber (heat cleaning and/or other cleaning methods)
- storage chamber for extra cathodes
- preparation chamber for activating cathode
- transfer mechanism between chambers and to the gun that must not generate any particles that can be transferred to the gun, nor ruin the vacuum in it

Figure 4.8 is a schematic of a simple but effective load-lock system that is mated to the gun shown in Figure 4.3. Each chamber has its own ion pump, and the cathode-preparation system also has non-evaporable getter (NEG) pumps to keep the vacuum low during activation and storage.

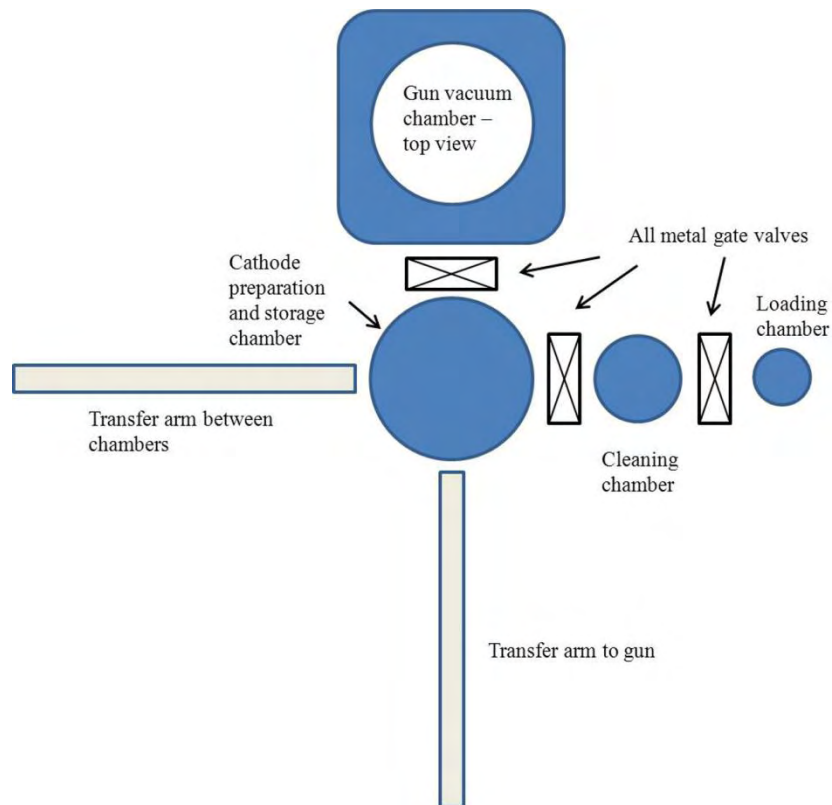


Figure 4.8. An example of a cathode load-lock system.

The load-lock chamber (Figure 4.9) has an internal quartz-lamp heater for performing a quick bake-out, and the volume of the load-lock is minimized to facilitate rapid pump-down. Once the vacuum is low enough in the loading chamber ( $< 10^{-6}$  Pa), both gate valves are opened and the transfer arm is pushed through to the loading chamber to pick up the cathode holder and move it to the cleaning chamber. Thereafter, both valves are closed and the wafer is heated to 580-600 °C for 1-2 hr. Some laboratories also use atomic-hydrogen cleaning as the first step [4.26]. After the cathode has cooled to room temperature (using a cold finger to hasten the process), the transfer arm picks up the holder and moves it to the cathode preparation chamber for activation.

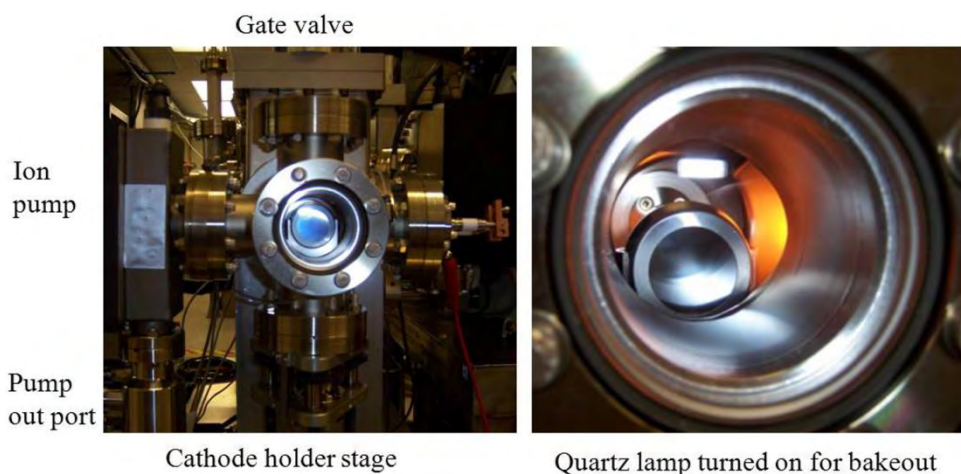


Figure 4.9. The load-lock chamber is shown on the left and a close-up of the system during a bake-out is shown on the right.

After activation, the valve between the gun and preparation chamber is opened and the transfer arm moves it into the gun, where it is registered and locked to the back of the electrode. There are numerous ways to secure the cathode, as long as the requirement of no particle generation is met. The materials in contact should be different to avoid cold welding. Molybdenum is used for the GaAs support and copper often is employed for the mating surface if heat must be removed from the cathode during operations. The arm is retracted, the valve closed, and then the gun is ready to go. Also, the cathode can be “topped up” if desired, by quickly retracting it, adding cesium, and then re-inserting it into the gun. During all of these procedures, the gate valve between the gun and the load-lock system should remain closed to reduce any chance of contamination, except when the cathode is removed from, or inserted into the gun.

At least two types of commercial transfer arms work well; one is a long, welded bellows, and the other a magnetically coupled rod. The former is somewhat more delicate of the two and requires care so as not to damage the thin-walled bellows. The magnetic type has internal bearings that potentially could produce particles, but the newest models generally are reliable in this respect.

#### 4.3.2.3 Vacuum Requirements

The use of semiconductor photocathodes and their reliance on low work function surfaces impose strict requirements on the vacuum conditions in the gun during operation. For GaAs cathodes in particular, vacuum levels  $< 1 \times 10^{-9}$  Pa are necessary for good cathode lifetimes. One particularly damaging phenomenon, ion back-bombardment, as discussed in Section 4.3.2.1, is best combated by reducing the vacuum level as low as possible.

Several methods will assure extremely low vacuum levels. The base pressure in stainless steel vacuum systems is dominated by hydrogen outgassing from the system’s thick metal parts [4.27]. It is preferable to

use SUS316L stainless steel for the vacuum chamber and all the flanges (and, in some cases, SUS316LN, if the flange must be brazed) to avoid any issues with stray magnet fields. For critical high voltage components, vacuum remelted stainless steel should be considered as it has fewer inclusions and contaminants that can cause field emission.

The hydrogen outgassing rate for stainless steel can be minimized by following the procedure described by Park [4.27]. All the stainless steel components should be baked in air (a vacuum bake is acceptable also) at 400 °C for 100-200 hours, followed by a 150 °C 24-hour vacuum bake after final assembly. This procedure is most effective on thin walled parts (a few millimeters), and less effective on thick flanges. It can reduce the outgassing rate to as low as  $2 \times 10^{-14}$  Torr L s<sup>-1</sup> cm<sup>-2</sup>. Note that titanium also was used successfully to produce low hydrogen outgassing rate chambers [4.28]. These rates can be lowered further by cooling the vacuum chamber walls, since the rate drops exponentially with temperature.

Only selected materials may be used in a gun, chosen for various mechanical-, thermal- and electrical-needs, including stainless steel, molybdenum, copper, alumina, or other pure metals (*e.g.*, titanium, tantalum, niobium and tungsten), plus the cathode material. Procedures for cleaning various materials are given in the literature [4.29] and many laboratories have their own standard procedures. Unfamiliar materials and coatings must be avoided without extensive testing; it is best not to trust recommendations from others without first conducting one's own tests.

The elimination of particles and dust is another critical process in preparing vacuum systems for high voltage guns. The SCRF community spent years perfecting particle-reduction techniques for superconducting cavities [4.30], many of which can be applied to guns. For example, the last step in cavity production is called high-pressure water rinsing (HPR). A moving jet of ultra-pure de-ionized water at  $7 \times 10^6$  Pa is sprayed on the surface of the niobium cavity for several hours and then allowed to dry in a clean room. The physical process is very effective in removing dust and contaminants that cause field emission. This process is applicable to most parts of the gun vacuum system before assembly. Even ion-pump chambers should be taken apart and cleaned with HPR. Section 4.3.2.4 gives an example with high voltage electrodes.

Another method for removing particles and quantitatively determining their contamination level is depicted in Figure 4.10 [4.31]. High-pressure gas (nitrogen or dry air) at  $5 \times 10^5$ - $1 \times 10^6$  Pa is sent through a 0.003 μm particle filter and then through a clean stainless steel hose and nozzle. The cleanliness of the filter, hose and nozzle first is checked by directing the flow into a particle counter and waiting until the count drops to near zero. Then, the object under test is sprayed with the high-pressure gas stream with the particle counter downstream. This process is continued until the particle count drops to near zero, which may take anywhere from a few minutes to hours, depending on the object's initial state of contamination. All of these procedures must take place in a cleanroom environment. This is an important final step before assembly, particularly for checking commercial parts, such as gate valves, that have many potential areas to trap particles and cannot easily be disassembled. Commercial CO<sub>2</sub> snow guns also can be used for this [4.32]; they utilize CO<sub>2</sub> as the gas and generate snow-like flakes that remove particles and degrease the surface.

Another technique to lower distributing particles from one place to another is to carry out the initial pump-down very slowly [4.33]. Evacuation rates of 5 000 Pa L s<sup>-1</sup> are slow enough to keep from stirring up particles and transporting them; this is accomplished using mass controllers and automated valves with inline 0.003 μm particle filters. Similar equipment is employed for venting the system.

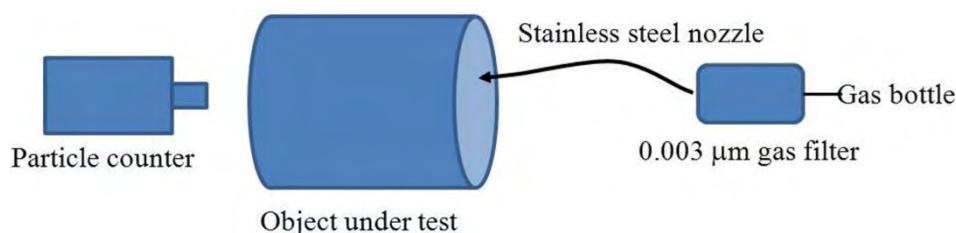


Figure 4.10. Set-up for removing particles from an object. Filtered gas is directed at an object, and the downstream particle count is monitored until it drops to near zero.

Even when using the procedures for hydrogen outgassing reduction, massive pumping still is required; often, an ion pump plus a large array of getter pump strips (such as SAES ST-707 [4.34], Figure 4.12) are used. The getters must be arrayed around the beam area as close as allowed by the high voltage hold-off tolerances. At low pressures, the pumps will be effective in the beam area only if there is a direct line of sight to the getters. The ion pump is needed for bake-outs and to pump methane and argon, which the getters do not pump well. Before installation, the getter strips should be rinsed in methanol to ensure that they are particulate-free. The getters are activated by heating to 450 °C for 45 minutes after system bake-out. Often, the release of gas during the activation can overwhelm the ion pump, so an external, baked, turbo station should be prepared should this happen. After the final bake and getter activation, a pressure  $< 5 \times 10^{-10}$  Pa routinely is obtained, with a typical post-bakeout residual gas spectrum shown in Figure 4.11.

Ion pumps are ineffective at very low pressures [4.35] and are difficult to restart at low vacuum levels if they shut off. Recently designed pumps have self-starters to keep them going, plus shrouds to block light and particles from escaping (Gamma Vacuum model 45S-IDIXTI). Turbo pumps and cryopumps typically are not used for photoemission guns since both types produce vibrations that can be transmitted to the cathode and cause beam motion. Also, mechanical devices require periodic maintenance, whilst ion pumps and getter pumps rarely do at the pressures involved. A cryopump recently developed by Oerlikon (COOLVAC BL-UHV) can be baked out completely; reportedly, it produces vacuum levels below  $1 \times 10^{-10}$  Pa, and thus may warrant further investigation.

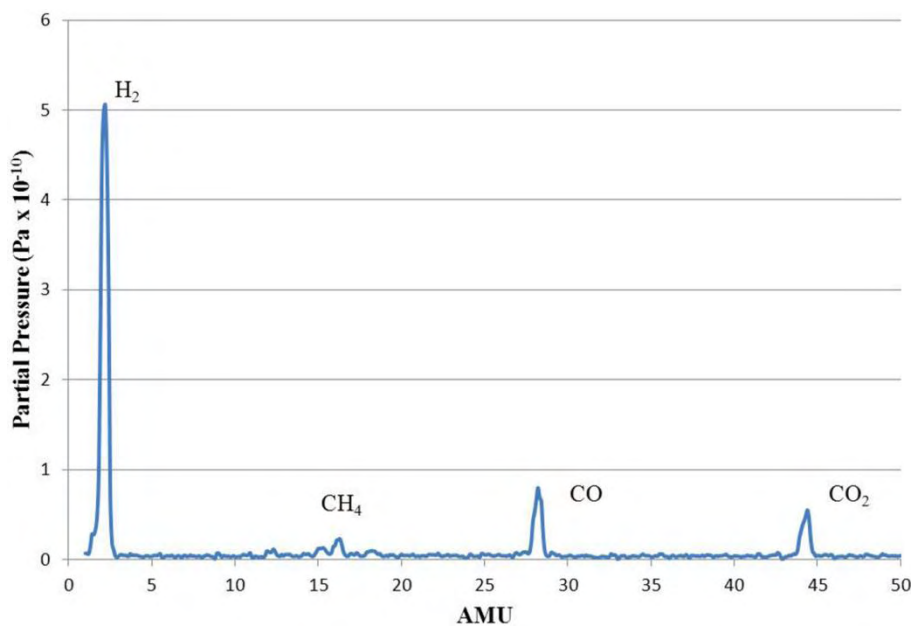


Figure 4.11. Residual gas spectrum after bakeout and NEG pump activation, showing hydrogen, methane, carbon monoxide and carbon dioxide. The total pressure measured with an extractor gauge was  $6 \times 10^{-10}$  Pa.

Another important consideration is the quality of the vacuum downstream (beamline) and upstream (load-lock) of the gun. The latter often is of good quality due to the needs of the cathode, but careful attention must be paid to anything that generates particles or introduces any gasses or materials into the gun during cathode preparation (especially cesium). Downstream of the gun, many components may be needed for manipulating and measuring the beam, introducing the laser, RF cavities for bunching and so forth. Each of these must adhere to the same standards as the gun chamber, and there must be adequate pumping. Insertable devices, such as view screens and gate valves, often are the worst offenders, as particles can be generated during motion. For machines where wakefields are an issue, these devices need to have RF seals (usually BeCu spring fingers) that also may produce particles. Individual parts should be pre-tested to avoid such problems.



Figure 4.12. An array of SAES ST-707 getter strips. They are connected in series to minimize the number of vacuum feedthroughs needed.

#### List of General Vacuum Rules

1. Use high quality materials.
2. Follow standard practices for UHV and cleanroom.
3. Avoid coatings and plating without extensive testing. The coatings may come off, producing particles. Instead of using plated screws (silver), use screws of different materials to avoid binding.
4. Chemically or ultrasonically clean all parts to remove surface contaminants and particulates. The cleaning process is material-dependent.
5. Pre-bake parts if possible to outgas them.
6. Design parts to eliminate virtual leaks.
7. Clean, store and assemble all components in a clean room.
8. Use filtered gas to remove particles, with a particle counter for monitoring progress.

#### Procedure for Cleaning Stainless Steel, High Voltage Electrodes

1. Machine to a surface finish of  $1 \mu\text{m rms}$ .
2. Use SiC paper to remove machining marks.
3. Rinse in methanol.
4. Ultrasonically clean in de-ionized water.
5. Store in water.
6. Electropolish, rinse and store in water.
7. Rinse with HPR for 4 hr to remove chemical residue then dry (in a clean room).
8. Air-bake at  $400^\circ\text{C}$  for 100 hr.

9. Rinse in HPR for 4 hr then dry (in a clean room).
10. Store until installation.
11. Blow with high pressure N<sub>2</sub> until particle count is near zero.

A final source of vacuum degradation is the dark current that generates electrons at high voltage surfaces. These can hit other parts of the vacuum chamber, thereby degrading the vacuum by electron-stimulated desorption of ions, electrons, atoms and light. Section 4.3.2.4 discusses the high voltage aspects of reducing dark current. Dark current problems related to the vacuum are minimized by cleaning and assembling the gun in a clean room to eliminate particle contamination. As mentioned in Section 4.3.2.1, carefully designing the cathode and focusing optics will eliminate stray electrons from the cathode, which can have a similar effect as dark current.

Improving the vacuum level is an important topic for photoemission guns and research needs to be continued.

#### 4.3.2.4 High Voltage Electrodes

As discussed earlier, the maximum charge that can be extracted from a cathode is determined by the electric field at the cathode and the laser spot size. Thus, much of the design work on various guns aims to make the electric field as high as possible (for both DC and RF guns). Also, if one can make electrodes that do not field emit, the demands on the insulator design are diminished – this is the Holy Grail for gun design (and for SCRF cavities). A few examples of DC gun electrodes are shown in Figure 4.13.

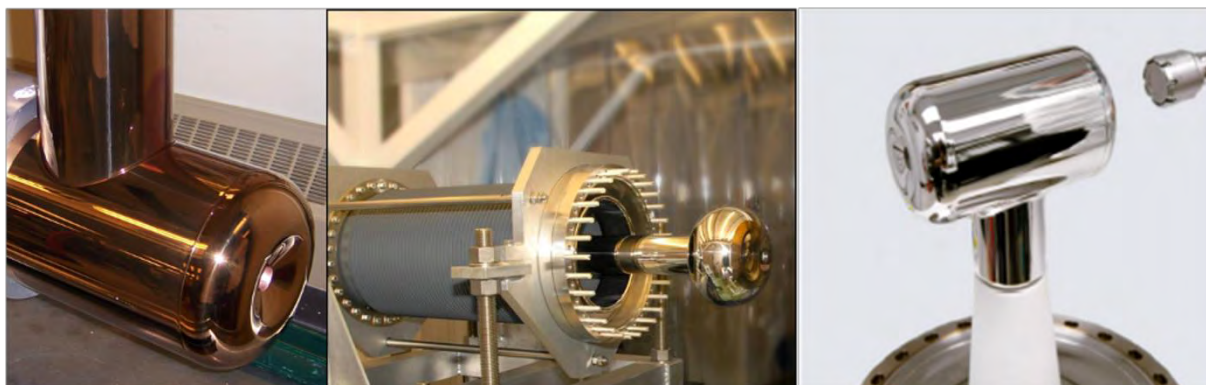


Figure 4.13. The focusing electrode for three different DC photoemission guns: the left picture shows the Cornell University stainless steel electrode, with the copper color resulting from an air bake to remove hydrogen; the central picture shows the gun used at Daresbury Lab [4.36] [credit to ASTeC, STFC Daresbury]; and on the right is the electrode used in the Jefferson Lab inverted polarized source. [Reprinted figure with permission from [4.37]. Copyright 2010 by American Physical Society.]

Volumes have been written about the best materials to use for electrodes, coatings to prevent field emission, cleaning procedures and geometries; unfortunately, most studies were for small anode-cathode gaps (millimeter range) and small-area electrodes. Incredible results were obtained that often led gun designers astray (myself included) when applying them to realistic geometries. The gun requirements covered earlier push toward the direction of very high voltages involving bigger gaps and large surface areas, which is not discussed often in the literature.

Figure 4.14 compiles data on HV breakdown for various size gaps [4.38]. For small gaps, the breakdown strength versus gap size is linear, but deviates from linear as the gap size increases. Hence, the experimental results from small gaps cannot be extrapolated to large ones. This phenomena often is called the “total voltage effect” [4.39], but the explanation is debatable. Additionally, this curve shows the breakdown

voltage for a gap. In a photoemission gun, the operation voltage must be well below the breakdown voltage to avoid field emission (which can cause electron stimulated desorption and vacuum increase, for example).

Figure 4.15 shows a test chamber for electrode studies used at Cornell University. Here, two large area ( $116 \text{ cm}^2$ ) electrodes with a Rogowski profile are held parallel to each other with adjustable gap spacing. The current hitting the anode is measured as a function of applied voltage (up to  $-125 \text{ kV}$ ), indicating the onset of field emission. A data set is displayed in Figure 4.16. Such a test stand is ideal for testing various materials for cathodes and anodes and for exploring new cleaning techniques. In this particular experiment, a stainless steel cathode was cleaned by different methods, resulting in a field of  $\sim 30 \text{ MV m}^{-1}$  for a  $4 \text{ mm}$  gap at  $125 \text{ kV}$ .

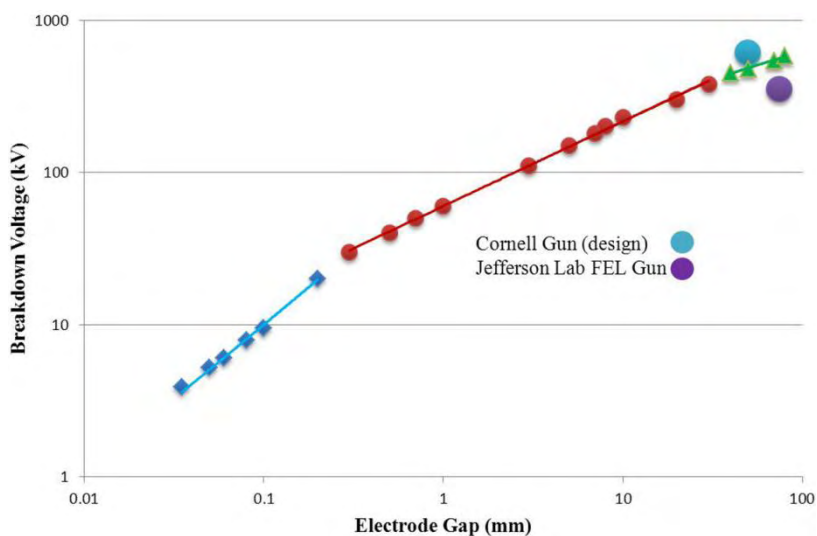


Figure 4.14. A compilation of breakdown voltage ( $V$ ) between electrodes for a given gap size ( $d$ ) from various authors [4.38]. The different colors indicate regions where the data range follows the displayed transfer function. The points for the Jefferson Lab FEL gun and the Cornell ERL gun are shown.

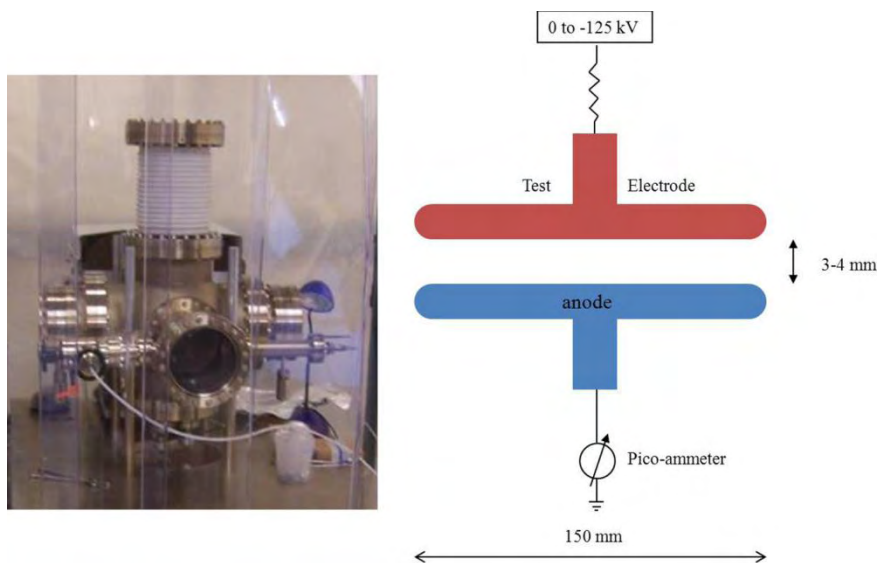


Figure 4.15. Test chamber for measuring the field emission characteristics of large area electrodes.

Extrapolating to  $500 \text{ kV}$ , a  $16 \text{ mm}$  gap for a large area electrode would seem achievable. Unfortunately, the best designs typically work at  $5\text{-}10 \text{ MV m}^{-1}$  or less for  $50 \text{ mm}$  gaps, far from the small-gap results. Two

important lessons emerge from this information: (1) While the findings from small area, small gaps can provide useful data, do not rely on them solely for realistic design parameters; and, (2) perform electrode tests on full-sized models.

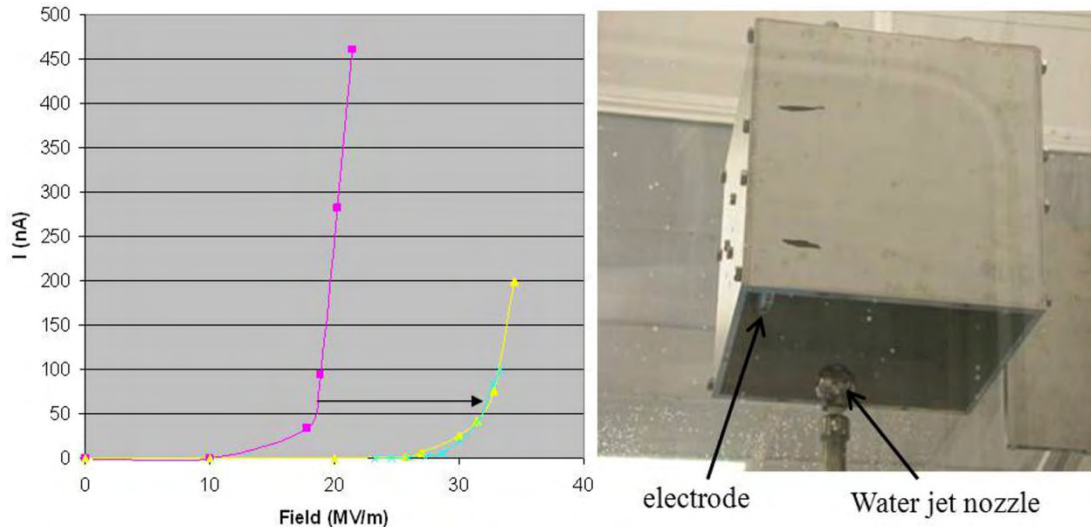


Figure 4.16. Results from field emission tests (left). The pink curve shows the current hitting the anode as a function of electric field for a 4 mm gap, hand-polished stainless steel sample. The green and yellow curves show the improvement after high pressure rinsing the electrode (green was originally hand polished, yellow was originally electropolished, 4 mm gap). The HPR fixture is shown on the right.

Figure 4.17 illustrates a chamber for testing large electrodes at large gaps that was constructed, in part, to study the total voltage effect [4.40]. The authors suggest that at higher voltages, the field-emitted electrons from the cathode can penetrate deeply into the anode, where eventually enough energy builds up to cause a catastrophic event. Such component-level test systems are crucial for gaining the necessary understanding for design very high voltage photoemission guns.

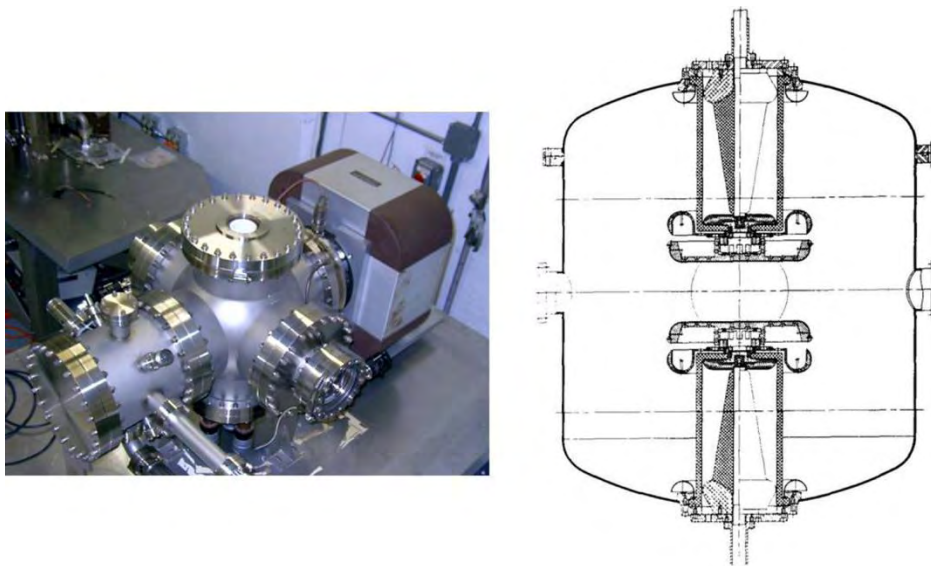


Figure 4.17. Vacuum chambers for investigating the “total voltage effect” on large electrodes. The chamber on the left can reach -250 kV on the cathode (anode grounded), while the system at the right can reach 600 kV (cathode at -300 kV, anode at +300 kV). [[4.24]; Available under Creative Common Attribution 3.0 License ([www.creativecommons.org/licenses/by/3.0/us/](http://www.creativecommons.org/licenses/by/3.0/us/)) at [www.JACoW.org](http://www.JACoW.org).] [[4.40] (© 1996 IEEE)]

Several groups are investigating the best material to use: Niobium, stainless steel, or molybdenum for cathodes, and titanium or beryllium for anodes show promise [4.21], [4.41]. The gun in Figure 4.3 has a cathode of stainless steel with a beryllium anode. Using beryllium for the anode has two advantages: Excellent thermal conductivity to remove the heat produced during field emission events; and, low atomic number to reduce the production of X-rays when struck by field-emitted electrons from the negative electrodes [4.21]. Many authors have detailed research on field emission (*e.g.*, [4.39]); it is not further discussed here.

#### 4.3.2.5 Insulators

Designing insulators for very high voltage DC photoemission guns is difficult. Many experts on high voltage engineering focus on pulsed power systems [4.42] that are not directly applicable to the DC case. Early work on large DC accelerating columns (Van de Graaffs) is not directly applicable, due to the special requirements for photoemission guns. Industrial devices, such as X-ray tubes for inspection work at 450 kV, operate in a bipolar geometry, with the anode at 225 kV and the cathode at -225 kV, and thus are not applicable.

In DC photoemission guns (Figure 4.3), the electrons must be accelerated quickly to high energy after leaving the cathode to reduce the effects of space charge. Accordingly, the anode-cathode gap should be minimal, both to increase the electric field on the cathode surface and to accelerate the bunches in a short distance. These requirements eliminate many successful older HV accelerating tube designs (Figure 4.18) because they lack a central support tube for holding the cathode close to the anode and their small diameter precludes inserting a tube while maintaining a reasonable field gradient. In these, the beam travels the length of the tube, gradually accelerating to the desired energy, and so is unsuitable for high bunch charges.

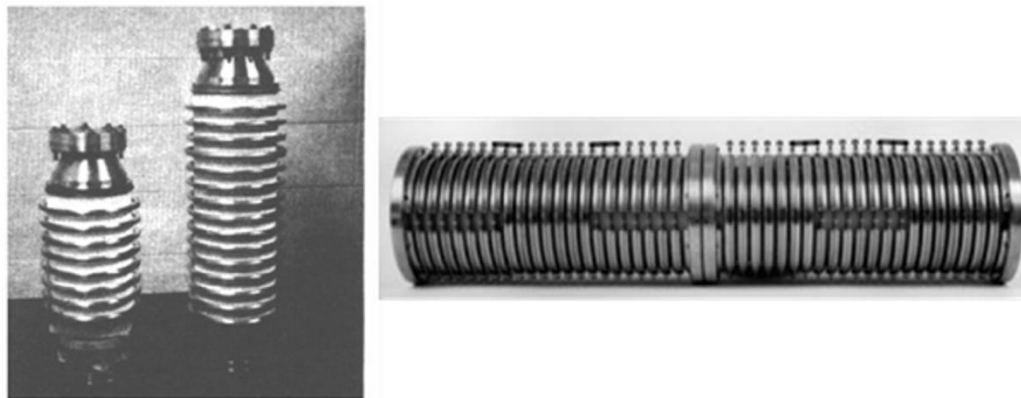


Figure 4.18. 300 and 550 kV accelerating columns (left), and a 1 MV accelerating column (right) from NEC. [[4.43] (© 1975 IEEE)]  
[Courtesy of National Electrostatic Corp.].

Since the insulator provides part of the vacuum envelope for the electron gun, the level of vacuum required (often set by the cathode type) greatly influences the insulator's materials and design. Here, I discuss the design covering the most difficult case of using GaAs-like photocathodes, which require a vacuum of  $< 1 \times 10^{-9}$  Pa. It eliminates many materials and sealing designs; O-ring seals cannot be used, nor insulators made from plastics or epoxies. To obtain such a good vacuum means that the device must be bakeable at high temperatures. Alumina is the most common insulator material used today.

Alumina comes in several different types, with the alumina content varying from 92% up to 99.5% (sapphire is 100% alumina, for comparison). The material properties change slightly with alumina content, but for high voltage applications, values in this range are reasonable. For RF window applications, 99.5%

alumina is often used due to the low RF loss factor. Table 4.4 lists the important properties. Several companies produce large alumina parts: CoorsTek; Kyocera; Friatec; SCT; and, Morgan Advanced Ceramics.

Property	92%	96%	99%	99.5%
Compressive Strength [MPa]	2 300		2 160	2 350
Tensile Strength [MPa]	180	193	241	
Young's Modulus	280	320	360	370
Thermal Expansion [40-800 °C, $\times 10^{-6} \text{ }^\circ\text{C}^{-1}$ ]	7.8	7.9	8.0	8.0
Thermal Conductivity @ 20 °C [ $\text{W (m K)}^{-1}$ ]	18	24	29	32
Dielectric Constant	9.0	9.4	9.9	9.9
RF Loss Factor ( $\times 10^{-4}$ ) @ 1 MHz	54	38	20	10
Volume Resistance @ 20 °C [ $\Omega \text{ cm}$ ]	$> 10^{14}$	$> 10^{14}$	$> 10^{14}$	$> 10^{14}$
Volume Resistance @ 300 °C [ $\Omega \text{ cm}$ ]	$10^{12}$	$10^{10}$	$10^{10}$	$10^{13}$

Table 4.4. Properties of alumina with varying alumina content.

To assure vacuum integrity, the insulator must be brazed to a metal ring that then either is brazed or welded to a vacuum vessel or vacuum flange. There are numerous examples of braze-joint geometries [4.29], brazing techniques and materials. Figure 4.19 shows a particularly good joint for the large insulators often used for photoemission guns. Many geometries that work fine for smaller diameters (200 mm and less) do not scale well as their dimensions increase with voltage due to the thermal expansion of various materials compared to alumina. Kovar offers the closest match for expansion versus temperature to alumina, and hence, is often used, however, it can become magnetized, so care is essential when low magnetic fields are required (electron microscopes, for example). Copper is often used even though the thermal expansion mismatch is much greater. The compressive- and tensile-strength of alumina is another important factor in designing a good braze joint. Alumina is ~6-8X stronger in compression than tension, so, after brazing, the joint should be in compression at its operating temperature. Figure 4.19 depicts a kovar braze-ring that is sandwiched between two cylindrical alumina rings, a geometry applicable to a single, large ceramic bushing, or a series of stacked ceramic rings. At the top and bottom, the kovar ring mates up with a vacuum chamber or flange, so that the two pieces can be welded to form the final vacuum seal. The bottom alumina ring helps equate the stress from brazing equally on both sides of the joint and affords a surface for registration with the vacuum flange. The stainless steel vacuum flanges should be treated to remove hydrogen before they are welded.

Finally, a vacuum bake (150-250 °C) and leak check should be undertaken. Surrounding the entire device with a large bag of helium will ensure the detection of the smallest leak. An RGA with an electron multiplier should show no helium signal above background after 1 hour.

An insulator must be able to hold off the maximum voltage applied without breakdown across its surface. Breakdowns occur on the vacuum side and the non-vacuum side, as discussed in [4.39]. The non-vacuum side can be air, SF<sub>6</sub>, oil, or even a solid dielectric plastic/epoxy. The insulator's environment determines the size and geometry that will prevent breakdown. In Figure 4.27, with  $4 \times 10^5$  Pa of SF<sub>6</sub>, 30 cm affords a conservative buffer to hold off 750 kV between the gun and the grounded pressure vessel. In perfect conditions with uniform electric fields, SF<sub>6</sub> can hold-off  $8.9 \times 10^{-4} \text{ kV cm}^{-1} \text{ Pa}^{-1}$ , but this is de-rated for practical situations. In air, the distance would be at least 2.5X larger. Oil is widely used in industrial devices, but is not recommended near UHV systems because of the potential for hydrocarbon contamination. Instead of placing the gun and power supply in a single tank, high voltage cables and

connectors can be used with the gun and supply located in separate tanks; they are readily available only up to ~225 kV [4.44]. Cables and connectors for higher voltages can be obtained [4.45] or made in-house, but their design is difficult and can lead to reliability problems.

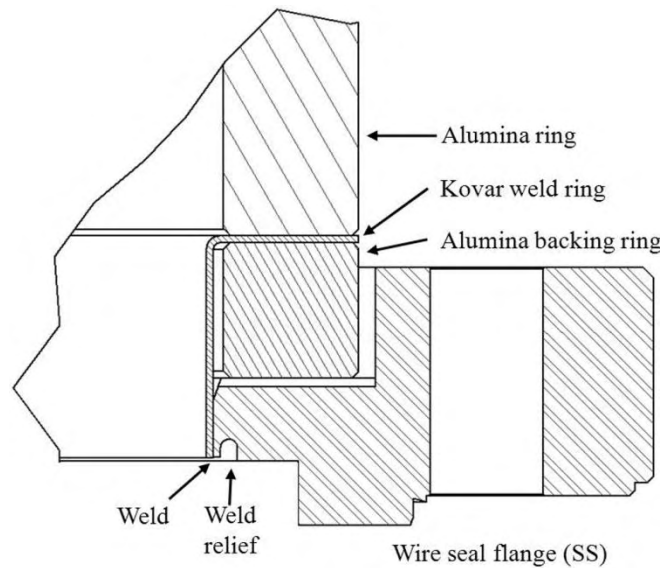


Figure 4.19. Braze design for a large diameter insulator. A kovar ring is brazed between two alumina rings and ring is welded to the stainless steel flange.

A rough estimate of the required insulator diameter can be found by using the formula for a coaxial cylinder

$$E = \frac{V}{R_{inner} \ln\left(\frac{R_{outer}}{R_{inner}}\right)} \quad (4.4)$$

where  $V$  is the voltage on the central conductor,  $R_{outer}$  and  $R_{inner}$  are the respective radii of the outer- and inner-conductor, and  $E$  is the electric field on the inner conductor. Since the outer conductor is part insulator and part conductor, this formula does not strictly hold and simulations are needed for the final design. A good upper limit for  $E$  is  $10 \text{ MV m}^{-1}$ , with lower values being better. For 750 kV, values of  $R_{inner} = 50 \text{ mm}$  and  $R_{outer} = 220 \text{ mm}$  result in a field of  $10.1 \text{ MV m}^{-1}$  on the inner conductor.

An insulator height of 250-300 mm is typically sufficient for 100 kV in air, or for 250 kV in  $\text{SF}_6$ . For 500 kV, 500-600 mm is adequate depending on the gas pressure. Again, simulations are needed to calculate the exact fields for the final geometry to ensure predetermined limits are not exceeded.

Important design considerations are the following:

1. Ensure ceramic parts are under compression.
2. Protect triple point junctions (limit the field to  $\ll 1.0 \text{ MV m}^{-1}$ ).
3. Make the diameter large enough to keep the central tube's field  $< 10 \text{ MV m}^{-1}$ .
4. Use sandwich-type braze-joints for large diameters ( $> 200 \text{ mm}$ ).
5. Ascertain that no magnetic materials are near the beam.
6. Make braze joints accessible so any braze overflow can be cleaned up.

7. Minimize designs and materials that can generate and/or trap particles.
8. Consider the mechanical strength under vacuum and SF<sub>6</sub> loading and how it affects mechanical alignment and tolerance for placing electrodes.
9. Confirm resistance to flashover, field emission, UV, thermal stresses, secondary emission and corona, any of which can affect the vacuum and impact cathode lifetime.
10. Braze in a vacuum furnace, not a hydrogen furnace.

All guns of the type described incur the problem of controlling field-emitted electrons leaving the high voltage surfaces. These electrons can land on the insulator, and if the charge builds up there may be a punch-through, causing a vacuum leak (Figure 4.20). Alternatively, or additionally, if heat builds up where the electrons strike the ceramic, the insulator can locally overheat and explode, also causing a leak [4.46]-[4.48].

A common design idea to bleed off these electrons is a cylindrical alumina bushing with an internal resistive coating. At high DC voltages, this was successful only up to 450 kV during processing, above which punch-throughs occurred [4.49]. The thin coating used in the reference exhibited a strong non-linear drop in resistance with voltage and the related increase in current passing through the ceramic can lead to thermal runaway. Further, the coating did not adhere well, leaving a layer of dust on the electrodes, certain demise for reaching 750 kV. Others adopted ion implantation to provide some conductivity [4.50]. For high voltages (> 300 kV), the electrons have enough energy to penetrate fractions of a millimeter into the material, beyond any thin surface layer. Thus, alumina with bulk conductivity is more desirable for higher voltages.

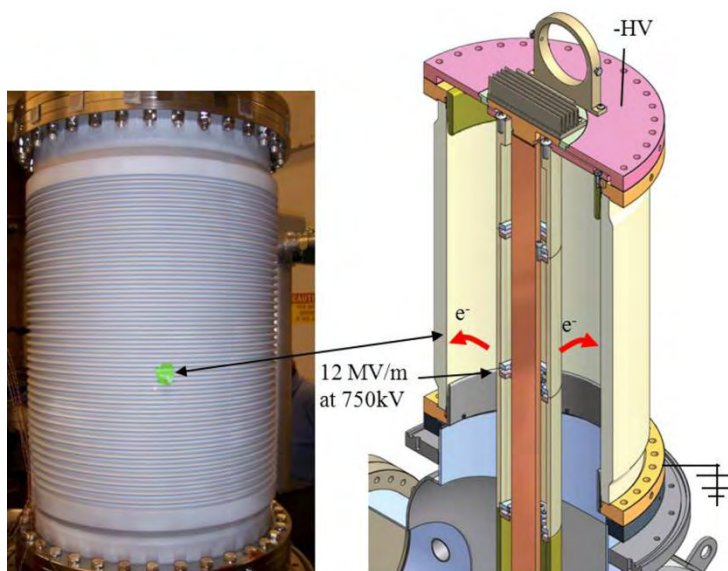


Figure 4.20. Insulator damage due to field-emitted electrons from the HV center conductor.

An insulator made from an alumina composite material from Morgan Advanced Ceramics (AL-970CD) was built at Daresbury Laboratory [4.36] that is resistant to field-emitted electrons up to 500 kV. It has a resistivity of 65 GΩ cm at room temperature that remains constant with changes in voltage. For the ~500 kV insulators discussed, this results in an overall resistance of 25-50 GΩ and draws 10-20 μA, limiting any potential thermal runaway. The same material was used at Cornell for a 750 kV gun, but it failed at 450 kV (Figure 4.21). The importance of using a slightly conductive insulator is still an open question, as another

failure mechanism for this system was discovered recently (section 4.3.2.7). If that turns out to be the root cause, this gun geometry may be able to reach higher voltages.

An alternative insulator, similar to an old accelerating tube, will completely block the line of sight between the electrodes and the insulator, thus preventing any field-emitted electrons from reaching it; such a device has been successfully tested to 550 kV [4.51]. Figure 4.22 and Figure 4.23 show a design for 750 kV.



Figure 4.21. A failure on a conductive insulator; the hole is  $\sim 1 \text{ mm}^3$  on the external surface.

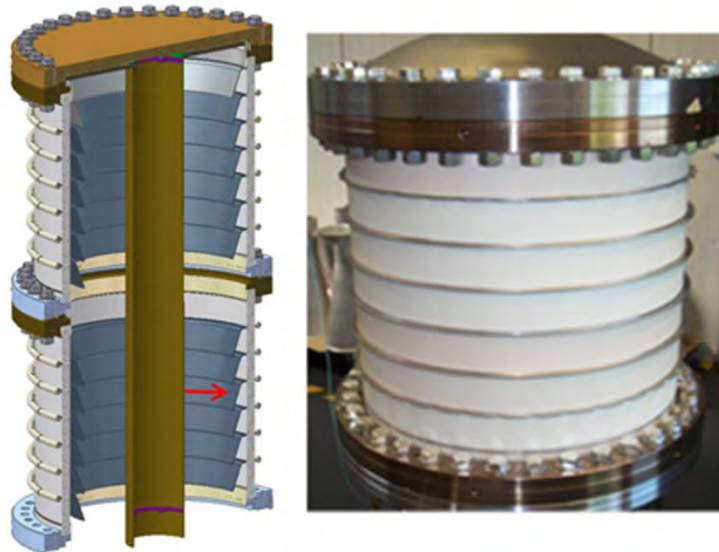


Figure 4.22. A segmented insulator design. The wire seal flanges have a 560 mm outer diameter and the insulator rings are 50 mm tall and 20 mm thick. Any electrons field emitted from the central tube (red arrow) are intercepted by one of the metal rings. The photo on the right shows one of the insulator halves. [[4.49] (© 1996 IEEE)]

The sizes were selected to keep the maximum field below  $10 \text{ MV m}^{-1}$  and triple point junction fields below  $1.0 \text{ MV m}^{-1}$  at the full 750 kV. The number of intermediate rings was chosen to limit the voltage between each ring to  $\sim 50 \text{ kV}$ , where external resistors maintain a uniform voltage from the top to the bottom of the device. The central support tube was sized to minimize the gradient on the tube. If desired, the complete insulator can be made in two pieces to improve manufacturability and to provide a location for mounting an intermediate electrode. The angle and length of the intermediate rings were chosen by simulations so that any electrons emitted from the high voltage surface of the long central-support tube would strike the rings and never reaching the alumina (Figure 4.22). There is also a likelihood that field emission between the rings will produce electrons that could land on the alumina, but they will be limited to 50 kV energy; the field gradients are low enough that field emission should be minimal. Kovar was used for the ceramic-to-metal joints for ease of brazing; any residual magnetic fields from the kovar will be far enough away not to affect the electron beam. The thermal conductivity of the material of the angled electrodes should be high

enough to conduct away heat from field emission, such as copper. The tradeoffs of strength, vacuum properties, secondary emission yield and HV properties will determine the choice.

Although this design has the best chance for success at very high voltages with excellent reliability and low dark current, it has several disadvantages. Its large size (to keep the maximum field below  $10 \text{ MV m}^{-1}$ ) necessitates very careful attention to cleanliness (particle reduction) and adequate pumping. Its large surface area at high voltage affords opportunities for field emission. A carefully designed external resistor chain is essential for maintaining the voltage at each ring, and for handling arcs during processing. Arc protection requires varistors or spark gaps between each ring.

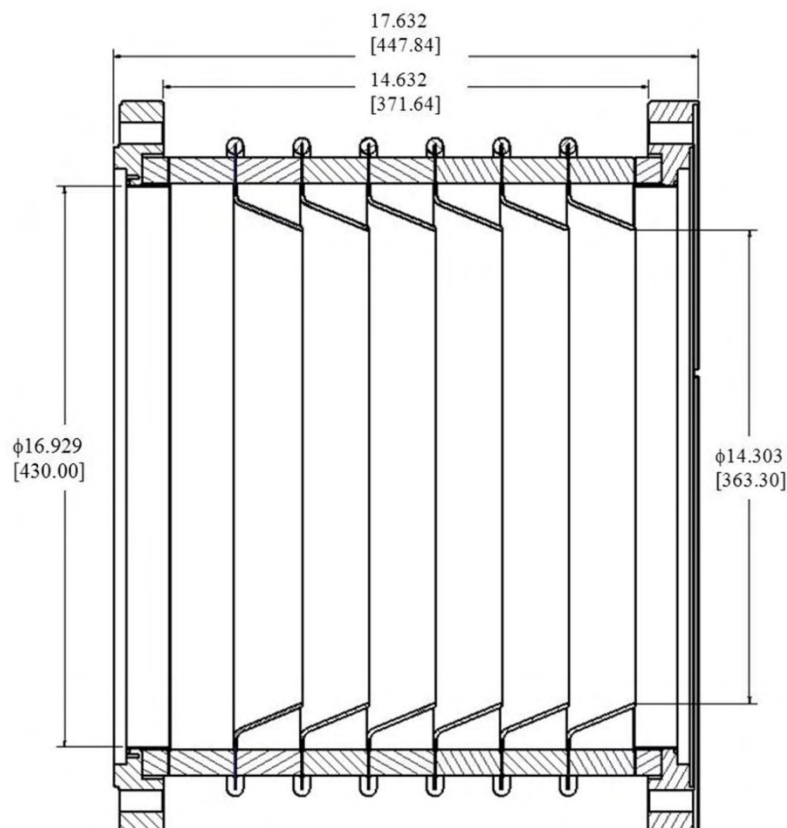


Figure 4.23. A 2-D drawing of one section of the 750 kV segmented insulator. The dimensions are in inches and millimeters. The inner rings are at an angle of  $23^\circ$  to the insulator's surface.

Another approach is adapting the design of an industrial X-ray tube insulator, rather than the bushing design. These are much smaller conical insulators with the cathode directly attached to the end of the cone, as Jefferson Laboratory demonstrated [4.37] (Figure 4.24). The following are its main advantages: less surface area at high voltage (correspondingly, fewer field emission sites); commercial components that work up to 225 kV; low vacuum chamber volume; and availability of mating HV cables. Higher voltage inverted guns will require substantial redesign effort to assure reliability [4.52].

Procurement poses a final difficulty with HV DC insulators. Companies with the necessary expertise may be uninterested in making small quantities, and so the final cost can be high and delivery time long. Such constraints encumber building and testing multiple configurations. Prototypes using plastic or epoxy materials for the insulator might be possible. Rexolite is a common material in pulsed-power insulators. While vacuum constraints preclude them for the final design, they are adequate for quick prototyping.

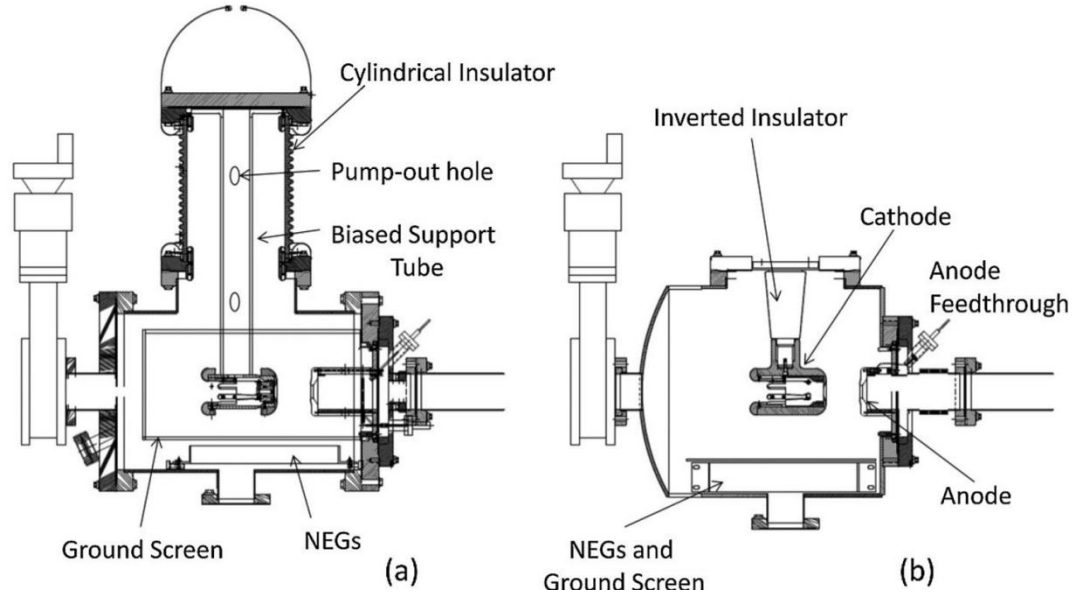


Figure 4.24. (a) A polarized source using a bushing-type insulator design and (b) an inverted insulator design. [Reprinted figure with permission from [4.37]. Copyright 2010 by the American Physical Society.]

#### 4.3.2.6 DC HV Power Supplies

The high voltage power supply for a DC photocathode gun is an important, but often overlooked component of the complete system. A sound set of requirements should be developed before considering what power supply to obtain. Table 4.5 lists many of the important requirements and representative values for a photoemission gun operating at 600 kV, 100 mA. Several of them are described later in the section.

The first item to determine is the highest voltage needed for routine operation and the overhead for conditioning. For stability, all HV electron tubes must be conditioned above the nominal voltage. Photocathode guns, particularly those using vacuum-sensitive cathodes, often require additional margin (up to 25%) for good cathode lifetime. Dark current (from field emission) in the nanoampere range is enough to produce noticeable local heating and light (X-rays and UV), contribute to secondaries and increases in pressure; a higher margin normally reduces the field emission at the operating voltage. For example, if 500 kV is the desired operating value, 600 kV would provide the minimum acceptable overhead.

For any gun that injects a beam into an RF accelerator, the control of the arrival time, or phase jitter, of the electron bunch is of critical importance. In terms of variation in gun voltage, the phase change  $\phi$  at a distance  $L$  away from the gun is given by

$$\Delta\phi = 2\pi f \frac{L}{c} \frac{\gamma - 1}{(\gamma\beta)^3} \frac{\Delta V_{gun}}{V_{gun}} \quad (4.5)$$

where  $\phi$  is in radians,  $f$  is the RF frequency in Hertz,  $L$  in meters,  $c$  the speed of light,  $\beta c$  is the electron velocity,  $\gamma$  the Lorentz factor,  $V_{gun}$  is the gun voltage in volts, and  $\Delta V_{gun}$  is the magnitude of the voltage ripple. In terms of the RF phase, variations of the order  $\pm 1^\circ$  are acceptable for low emittance beams. For example, at  $f = 1.3$  GHz,  $\Delta\phi = 1^\circ$  corresponds to a shift of  $\pm 450$  V, 1 m away from a 250 kV gun (0.18% variation). At 500 kV, the allowed variation increases to  $\pm 1640$  V (0.33%). The voltage variation, commonly called ripple, must be specified over the frequency ranges in the power supply, typically up to 60 kHz (or more) for modern switching supplies.

For a particular power supply, even monitoring ripple at the levels required, particularly higher frequencies, may be difficult. A time-of-flight detector (a beam-position monitor, for instance) downstream from the gun can be used to monitor the arrival time of the electron bunches. These devices easily measure the arrival time with sub-picosecond accuracy at many tens of kilohertz; the resulting signal is sent back to the power supply's feedback control loop. Both long term drifts (thermal) and short term variations (ripple) can be corrected to maintain a chosen arrival time at the detector. For known problem frequencies or instabilities in the HV power supply, feedforward methods might be useful.

Parameter	Specification	Notes
Operating Voltage	400-600 kV	
Conditioning Voltage	750 kV	
Maximum Current	100 mA	
Ripple	$\pm 0.2\%$ at 500 kV	Value depends on the gun voltage
Voltage Reproducibility	0.2% after 1 hr	
Ramp-up Time to Full Current	50-100 ms	Depends on RF control system bandwidth and cavity fill time
Personnel Safety	At least 2 independent interlocks must be satisfied before turn on	
Machine Safety	Should have an external signal to shut down if an accelerator trip	
Arc Detection	A $dV/dt$ circuit to sense an arc and trip the supply	
Temperature Stability	0.01% of volt per 1 °C	SF <sub>6</sub> temperature can be regulated, if needed
Environment	100% SF <sub>6</sub>	Can use mixtures of N <sub>2</sub> and SF <sub>6</sub>
Current Measurement	Ability to measure with $< 1 \mu\text{A}$ resolution for HV conditioning of electrodes	Need to separate the load current and the internal PS current draw
Calibration	1% of full scale	Using external divider, difficult at this voltage and in SF <sub>6</sub>
Current Limit Trip	Exceeding preset limit trips the supply	
Line Regulation	$V_{out} \pm 0.5\%$ for a $\pm 10\%$ line variation	
Voltage Stability	0.25% from 10-100 mA	
	DC output $\pm 0.4\%$ over an 8 hour period, including ripple	
Capacitance/Stored Energy	100 pF, 10 J	Not a firm number, but lower is better
External Feedback Port		Ability to apply an external signal to superimpose on control loop

Table 4.5. Specifications for high voltage power supply.

Current stability and the response of the voltage to changes in the current are of utmost importance for photocathode guns. Drive lasers should be stable in power to  $< 1\%$ , so the HV output should be insensitive to such changes in current level over a wide frequency range. As the cathode efficiency drops over time, laser power must be increased correspondingly to maintain output constant.

Another concern for photocathode guns is how to ramp up the current to reach the maximum operating value. Two strategies exist: 1) Start in CW mode at low current and ramp up the bunch charge; or, 2) start a full bunch charge in pulsed mode and increase the duty factor until the CW mode is reached. Both methods are problematic. For the first case, focusing changes as the bunch charge increases, necessitating either adjustments of the optics settings to compensate, or choosing a less-than-optimal setting that works for the full range of bunch charges. The second case requires a flexible laser-pulse generation system that can handle the full laser power without damage for duty factors from 0-100%. Existing systems can be turned on directly to a few milliamperes without tripping the RF systems. Beyond that, the HV power supply must be able to ramp-up the current quickly (50-100 ms is desirable) while maintaining a constant voltage at low ripple. The actual ramp-up time needed will depend on the accelerator's size, the RF control bandwidth and the cavity fill time.

A precision voltage divider can assure absolute calibration of the power supply. This often is difficult to realize because the supplies are normally held in a pressure vessel containing  $\text{SF}_6$  or oil. The divider must be in the same vessel for the calibration. If absolute calibration is essential, the tank may need modification to leave the probe in place. For most photoemission guns, absolute calibration is not particularly important, but voltage repeatability and reproducibility are.

There are two types of DC supplies typically used in photoemission guns, and they cover the ranges of: lower voltage ( $< 225$  kV) for a wide range of currents (0 to 100s of milliamperes); high voltage, low current ( $< 10$  mA); and high voltage, high current (100 mA range). Staying at or below 225 kV is very convenient as it is the maximum voltage used in many commercial X-ray tubes. Above that range, the choices of commercial power supplies are very limited.

Cockroft-Walton voltage multipliers and variations thereof commonly have been used for many decades to produce voltages up to megavolts. The idea is simple [4.53], but implementation requires great skill to meet the strict requirements for photocathode guns (Figure 4.25 shows an example power supply).



Figure 4.25. 500 kV, 8 mA power supply (Glassman HV, Inc.) and  $\text{SF}_6$  tank used at Daresbury Laboratory [4.54]. [Credit to ASTeC, STFC Daresbury]

Industrial systems requiring high voltage and high current often use isolated core transformers (ICTs) [4.55]. Figure 4.26 is a schematic view of such a HV power supply. In contrast to the Cockcroft-Walton type voltage multipliers, ICT supplies distribute line-frequency power to individual multiplier sections *via* a ferrite core transformer. A motor-driven autotransformer varies the primary voltage, thus regulation is slow (tens of Hertz). Flux leakage at the higher sections reduces the voltage per turn on the secondary, requiring changes to the sections to compensate for the losses.

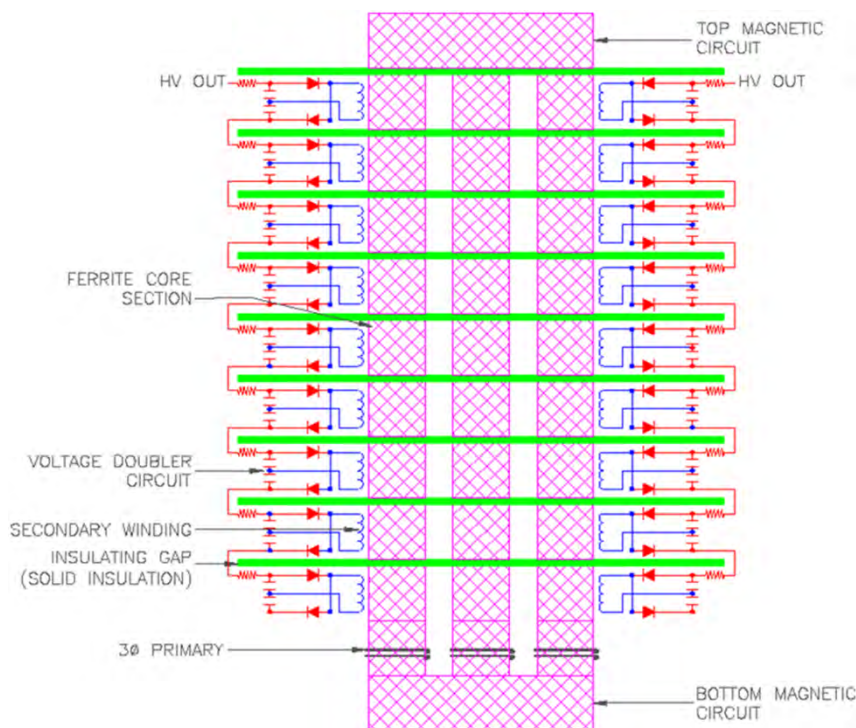


Figure 4.26. A schematic view of an isolated core transformer. [Reprinted with permission from [4.56]. Copyright 2009, American Institute of Physics.]

The Cross Transformer is a modern implementation of the ICT [4.56] that overcomes the limitations of an ICT, resulting in a very compact, convenient design for various accelerator systems. Its high-frequency PWM driver results in a much smaller footprint. A compensation capacitor corrects the flux-leakage problem so that each of the sections (circuit boards) is identical. The fault-tolerant individual multiplier sections are held at a low enough voltage to avoid corona, and the failure of one multiplier circuit on a board does not affect the entire board. The design has extremely low capacitance, resulting in low stored energy and a fast response time.

Figure 4.27 shows a -750 kV, 100 mA DC supply from Kaiser Systems, Inc., built using the Cross technology. The supply is very compact compared to other supplies operating at these voltages because all components are mounted on stacked-up printed circuit boards (Figure 4.28) to reach the desired voltage. Each board generates up to 12.5 kV and 100 mA, with 60 boards needed for 750 kV. The system is mounted in an SF<sub>6</sub> tank (pressurized to  $4 \times 10^5$ - $5 \times 10^5$  Pa) next to the electron gun.

The same supply can also be used for electrode conditioning when a suitable current limiting resistor is placed between the gun and the power supply (Section 4.3.2.7). The low stored energy (< 10 J) is an advantage for conditioning, as it limits the amount of energy that can go into a field emission site, reducing potential damage to the insulator and electrodes.

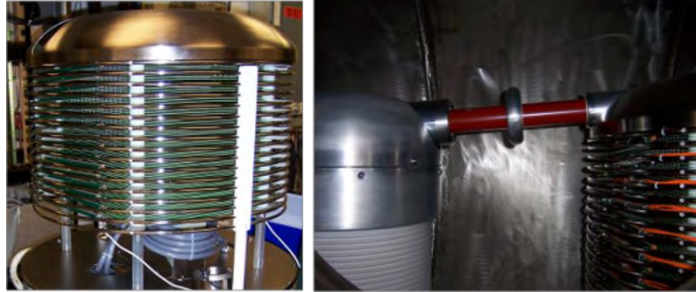


Figure 4.27. Kaiser Systems, Inc. high voltage power supply, producing -750kV at 100 mA (left). On the right, the power supply is connected to the top of the electron gun insulator. The orange wires are fiber optic cables transmitting signals from a floating ammeter measuring the current entering the gun. [[4.49] (© 1996 IEEE)]

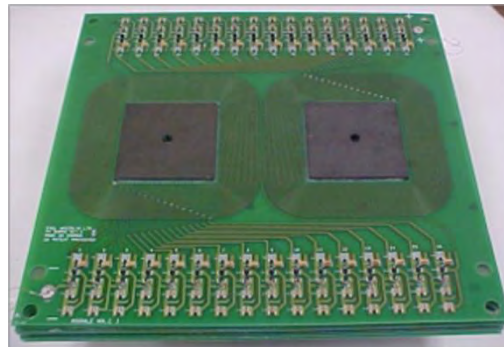


Figure 4.28. A 40 cm × 40 cm circuit board from the Kaiser Systems -750 kV supply. Each board can generate up to 12.5 kV and 100 mA. [Reprinted with permission from [4.56]. Copyright 2009, American Institute of Physics.]

#### 4.3.2.7 HV Conditioning

All high voltage vacuum devices must undergo an initial conditioning so that the device is stable during normal operations. “Stable” can mean different things for different systems. For example, an X-ray tube used in a CT scanner can typically have a few high voltage arcs per exposure, as the image-processing software can correct for any artifacts due to the arcs. However, for a photoemission gun, the use of extremely sensitive electron-emitters like GaAs means that no arcs can be tolerated. In addition, even very low-level electron field emission from electrodes can impinge on the vacuum chamber’s surface, generating X-rays, UV light and other particles that can increase the vacuum pressure and even damage the cathode’s surface. Many studies [4.39] have shown that high voltage hold-off capability of electrodes and insulators is influenced by dielectric thin films (oxides), electrically stressed interfaces (triple points), metallic- and non-metallic-particulates, absorbed gases and dielectric inclusions. Their various influences were studied extensively, especially for niobium superconducting RF cavities [4.30]. Material properties and cleaning methods to minimize inclusions and particulates are critical to success.

HV systems are processed in several ways, including *in-situ* heating to remove absorbed gases, conditioning with multiple breakdowns, plasma processing, gas conditioning and pulsed processing. For pulsed power machines, reference [4.57] provides an excellent review of the processing. Typically several different methods are used for photoemission guns, partly determined by the extreme-vacuum requirements. Since, often only one or two units are built due to their cost and complexity, developing the best conditioning procedures for the guns is difficult; great care must be taken not to damage them. In contrast, multiple models of industrial devices can be built and tested to establish optimum procedures.

The goal for processing is to operate at a given voltage while drawing a minimum amount of current from field emission sources on the electrodes, preferably picoampere levels, but no more than nanoamperes. The

lower the dark current, the more stable is the system, with fewer opportunities for vacuum bursts from electron-stimulated desorption. The processing voltage must be well above the operating point, typically 10-25%.

During processing, the gun vacuum is monitored with an extractor gauge (for total pressure), an RGA for measuring residual gas-content, arrays of photomultiplier tubes, Geiger counters for radiation, an accurate measure of the current from the power supply (with microamperes or better resolution), an arc counter, and perhaps an arc detector inside the SF<sub>6</sub> tank. The output of one or more of these monitors can be connected to interlocks for disabling the HV power supply. The power supply current limit should be set to ~100 μA. A low-capacitance HV power supply (described in Section 4.3.2.6) is beneficial in reducing stored energy, and thus the energy that can go into an arc (< 10 J is a good upper limit). A resistor between the gun and power supply limits the current to the arc with a value sufficient to always keep the current below a few milliamperes maximum. If the resistor is too large, processing will be very slow or non-existent; if too small, the electrodes and/or insulator may be damaged. Resistances of 50-200 MΩ often are used.

At the start of processing, the voltage is ramped up until there is a sign of activity, either an increase in vacuum, dark current, or radiation, which typically begins around 250 kV for the gun in Figure 4.3, or when gradients of 3-4 MV m<sup>-1</sup> are exceeded somewhere in the gun. Then, the voltage is increased in small steps (say 100 V) at a rate of 1-10 kV per hour. The rate is determined by keeping the vacuum level below ~1×10<sup>-6</sup> Pa, the dark current below a setpoint (< 100 μA) and the arc counter low enough to protect the resistors from overheating. The values determine how quickly the processing will proceed. Often, all the diagnostic signals will increase during an arc, but sometimes only one or two, depending on the source of the HV activity. When the signal(s) start going up, there are several methods for reacting. In the constant-current method, after the dark current jumps, the voltage is held steady until the current drops back to its baseline value before again stepping up the voltage. With spark processing, the voltage ramp is continued until either a discharge occurs, the dark current is knocked down, or one of the preset trip limits is reached. The procedure is very slow due to keeping limits on the allowed vacuum-pressure excursions.

Identifying a universally successful procedure is difficult because the type and location of field emission can vary depending on the cleaning methods, materials used, assembly procedures, *etc.* Even during processing, the system's response may change as the voltage rises, potentially requiring a different resistor value or new setpoints for the process variables. Field emission events can splatter material around the original emission site, generating multiple new sites requiring re-processing. Difficulties are compounded since only one or two guns are available and risks cannot be taken in assessing the best methods.

The vacuum level in the gun during processing warrants extra attention. Normally, the gun is vacuum baked after assembly and the NEG pumps activated, resulting in a vacuum level less than 10<sup>-9</sup> Pa. Absorbed surface gas is removed from the electrodes during bake which should shorten HV processing time. If the pressure becomes too high during conditioning, the good pre-conditioned vacuum levels for GaAs-like cathode operation may not be recovered. Re-baking to improve the vacuum will change the surface condition of the electrodes, usually necessitating further processing. As higher and higher voltages are reached, recovery from field emission-induced vacuum events is prolonged, as there is more energy per event, which increases surface heating. The RGA spectrum should reveal only H<sub>2</sub>, CO, CO<sub>2</sub> and CH<sub>4</sub>, with CH<sub>4</sub> typically taking the longest to pump away, as NEG's do not pump methane.

Sometimes, processing reaches a point where there can be no further progress without endangering some system component. Several laboratories have experimented with processing using noble gases, such as helium and krypton [4.24], [4.58]. Introducing one of them at  $\sim 10^{-2}$  Pa of pressure while the HV is on generates ions that either chemically react with, or damage field-emitter sites on the negative electrodes, quickly eliminating emission. A turbo pump, attached to the gun during this process, controls the pressure of the process gas. Since the getter pumps do not pump noble gasses, they do not become saturated. Although the ion pump is turned off to avoid overloading, it releases methane. Unfortunately, this process is “blind” to the residual gas content (other than the noble gas). It is easy to open up a vacuum leak without even knowing it. While this method is very efficient, more research is needed to verify its usage for the entire process. One problem is that a fix may not be permanent. If the gas absorbs or reacts with a particle on the HV surface, presumably raising its work function enough to kill the field emission, the gas eventually may desorb due to heat or other processing. Should the ion damage the emission site by melting, beneficial results will be maintained. After gas processing, regular processing can resume until another intractable spot occurs.

Guns of this type with cylindrical ceramic bushings are limited to well below the desired 500 kV operating points due to punch-throughs between 450-500 kV. Several insulator designs and coatings have been tried, and several new ones are ready. Another potential weak link in a HV system is the current limiting resistor used for processing.

The system (Figure 4.27) failed at  $\sim 450$  kV for several different insulators, no matter how carefully prepared, leading to the assumption that the insulator was the cause of the problems, not the effect. Recently, it was observed that each time the insulator experienced a punch-through, the current limiting resistor also failed. In fact, during an arc, the gun side of the resistor can drop to ground, resulting in the full voltage being dropped across the resistor, which was rated only for 40 kV continuous. After several such events, the resistor fails open, and seemingly, an arc occurs through the SF<sub>6</sub> gas across the resistor, dumping all of the power supply energy into the field emitter (tens to hundreds of Joules, depending on the power supply). The exact order of events is difficult to determine, but the resistor chain certainly was not designed properly.

The initial resistor used was a Cableform model CJE (40 kV, 35 W average power dissipation, Figure 4.29); they normally withstand 2.5X the power rating for up to 5 s, with 1.5X over voltage. So, during 5 s, 438 J can be dissipated and if the power supply dumps 100 J per arc, then the resistor can handle up to 4 arcs per 5 seconds. With two resistors in series, the value is 8 arcs per 5 seconds. Thus, to assure survival (and the over-voltage condition), only 8 arcs per 5 seconds are allowed. Hence, an arc counter is needed (dV/dt monitor); once the maximum arc rate is exceeded, the voltage must be reduced or turned off to allow the resistors to cool. The resistor chain also must be long enough to hold off the full voltage of the power supply during an arc. If the resistor is damaged (open), then a flashover could occur through the SF<sub>6</sub> if its length is too short. This particular design did not adhere to most of these conditions.



Figure 4.29. A high voltage resistor damaged during processing.

Multi-megaohm resistors that simultaneously withstand high voltages, high average power and multiple high-energy impulses are scarce. Nicrom Co. recently marketed very long thick film resistors capable of withstanding up to 400 kV in air continuously, with average power ratings up to 250 W, at the hundreds of megaohm range needed. The maximum energy a single resistor can withstand (assuming 2.5X surge power rating and 1.5X surge voltage rating for no more than 5 seconds), in 5 s is 3 125 J, or 31 arcs per 5-second period (100 J power supply). Adding several in parallel (Figure 4.30) raises this number and provides redundancy. In addition, the 1 m length affords a 600 kV surge hold-off in air and substantially more in SF<sub>6</sub>. For a conditioning supply with lower capacitance, the lower stored energy allows the resistors to withstand many more arcs per period.



Figure 4.30. Processing resistor schematic using three long resistors in parallel.

Lacking such high power resistors, series chains of smaller resistors can be employed, similar to the construction of high voltage dividers (see Figure 4.31). Caddock produces several reasonable high power, high voltage resistors, such as model MS-310 (1 M $\Omega$ , 10 W, 4500 V, 32 mm long body, 5X rated power with applied voltage not exceeding 1.5X rated for 5 s). Using 100 resistors in series gives 100 M $\Omega$  and 1 kW continuous power-dissipation (5 kW for 5 s, 450 kV \* 1.5 = 675 kV in air hold-off). Using 200-2 M $\Omega$  resistors in parallel offers redundancy.

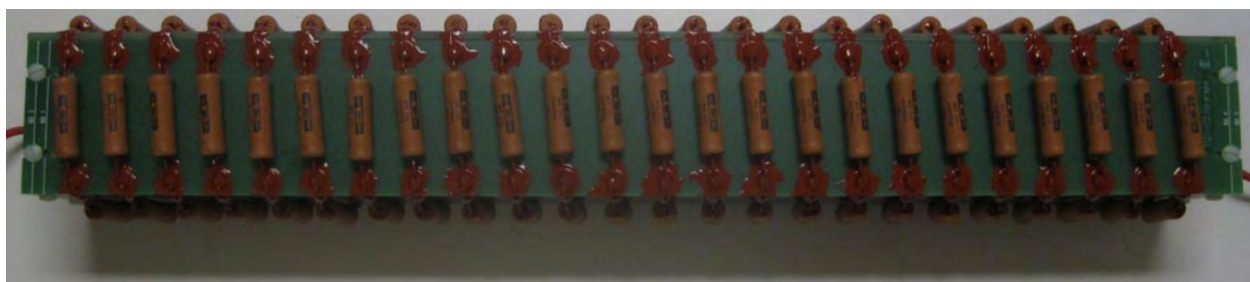


Figure 4.31. A processing resistor constructed from 100 individual resistors

While a poorly designed resistor is likely to be a major failure mechanism, other more robust insulator designs are being pursued presently.

### 4.3.3 Bunching and Focusing Section

The section after the gun has several functions: Focusing the beam to keep it from getting too large; focusing for emittance compensation; compressing bunches; diagnostics; and, focusing and steering into the first cavity of the cryomodule. The desire to shorten the distance from the gun to the cryomodule leads to a very congested beamline. One group [4.58] is planning considerable reduction by placing the gun directly inside the cryomodule (Figure 4.32). The advantage of limited distance must be weighed against lack of access to the gun, fixed focusing distance and no diagnostics.

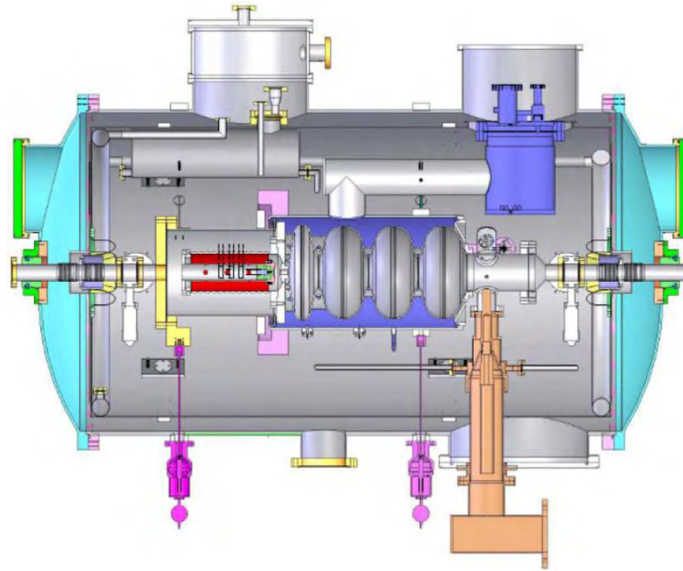


Figure 4.32. A combination DC gun/SCRF accelerator mounted inside a cryomodule. Such a design minimizes the possible drift distance after the anode. [[4.59]; Available under Creative Common Attribution 3.0 License ([www.creativecommons.org/licenses/by/3.0/us/](http://www.creativecommons.org/licenses/by/3.0/us/)) at [www.JACoW.org.](http://www.JACoW.org/)]

Figure 4.33 shows an example of a more typical focusing and bunching beamline. A pair of corrector coils placed directly after the anode allows centering the beam on the axis of the first solenoid. Having enough degrees of freedom for steering is important; thus, two sets of correctors before the solenoid are preferable, to correct for angle- and offset-errors. In this illustration, a second set of correctors is located inside the solenoid to save space, along with a beam-position monitor. An RF-sealed gate valve protecting the gun is sited between the gun and first solenoid, but could be placed after the first solenoid to bring the focusing element closer. Simulations can determine the best location for all elements. A laser input box is next after the solenoid, followed by a normal conducting buncher cavity, a view screen, an RF-sealed sliding bellows joint and a final solenoid/corrector/bpm package.

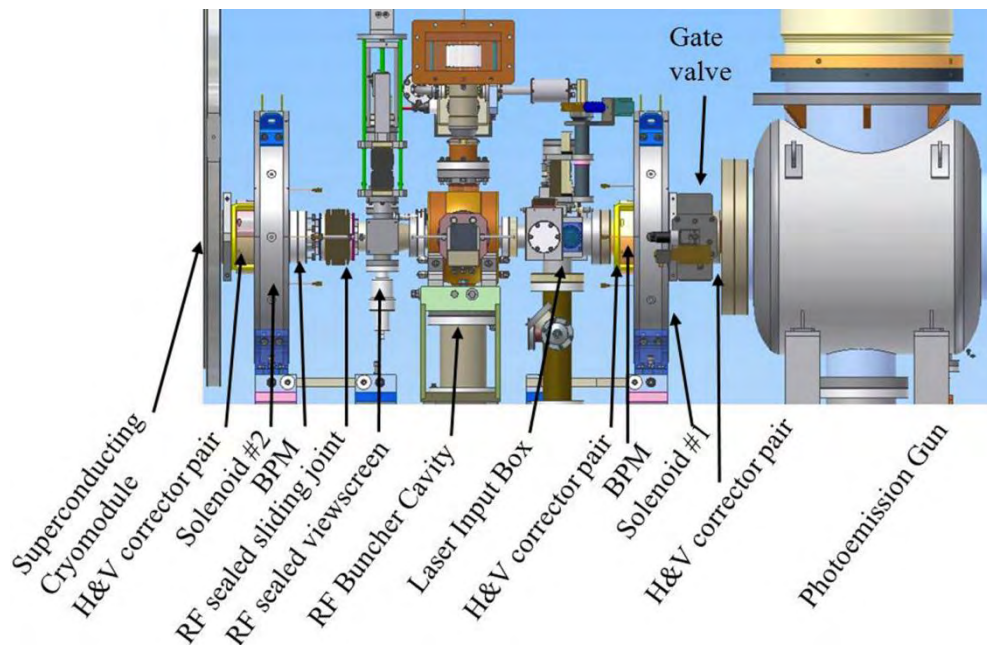


Figure 4.33. A bunching and focusing section between a DC gun (right) and a superconducting accelerating cavity (left).

The vacuum level in this section must be low enough that the gun vacuum is unaffected when the gate valve is opened, thus requiring strict adherence to the vacuum procedures for the gun. All of the moveable devices must be carefully designed and tested to minimize particle generation. For example, the tuners in the buncher cavity use BeCu spring fingers to maintain RF contact, but these scrape material from the tuner during motion. Coating the tuners with TiN eliminates this problem, and additionally, reduces RF multipacting.

To reach adequate vacuum levels, all parts should be heat-treated to remove hydrogen, and all designed to withstand bake-out temperatures of at least 200 °C. Similarly, the magnet coils must be potted with a high-temperature epoxy (such as Aremco Bond 526). Due to the limited conductance through the beam pipes, several smaller getter-pump cartridges are used, along with several ion pumps (the ion pumps must be magnetically shielded so they do not disturb the beam). Another option is to NEG-coat the interior of the beam pipes instead of using discrete getter pumps.

Solenoid alignment and the solenoid field quality are critically important for obtaining good beam emittance. Passing through an off-axis solenoid will cause asymmetric focusing across the beam and can affect the quality of the emittance compensation process. A remote control positioner can be used to put the solenoid on the same axis as the gun. One group reported how the quality of the solenoid field affects emittance [4.60]. They found the fringe-field region of the solenoid had a low-level quadrupole component, so they added correction coils to compensate for the irregularities, achieving a 10-30% drop in emittance.

The equations for ballistic bunching are well known for non-space charge dominated beams [4.61]. When space charge is important, the formulas provide only a rough estimate for the distance and power required to obtain the desired bunch length; simulations are needed to finalize the design. An example of a 1 300 MHz CW buncher (normal conducting) [4.62] is shown in Figure 4.34.

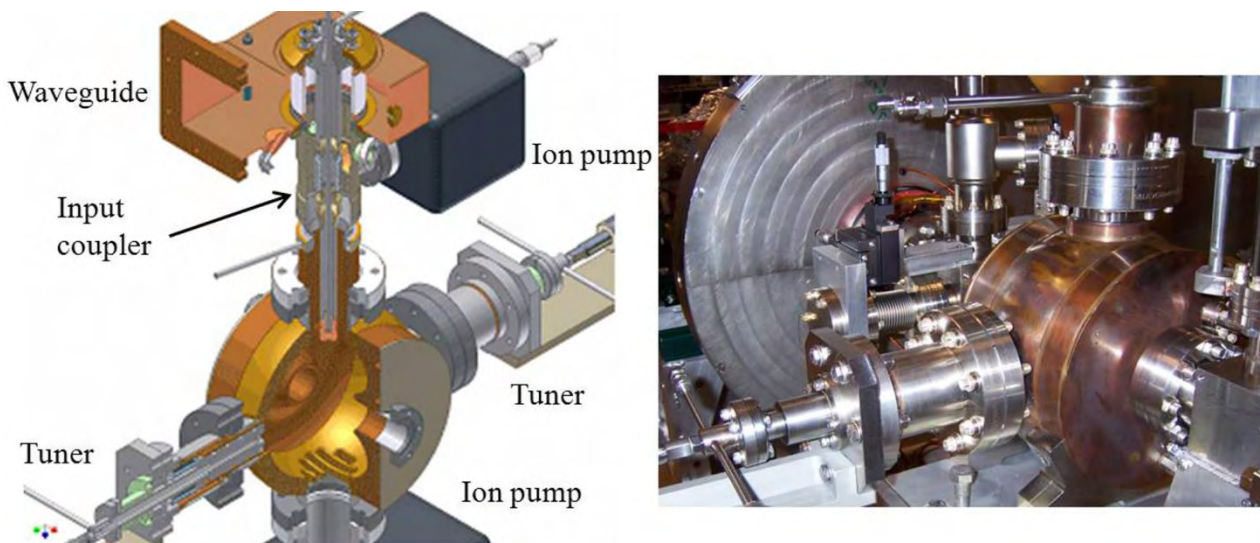


Figure 4.34. A schematic cutaway view of a CW RF buncher (left). The actual buncher cavity is shown on the right, with the laser box and focusing solenoid in the background.

Water-cooling is provided to the tuners, input coupler and the copper cavity. Compressed air blowing on the alumina RF window in the coupler keeps it cool. The water channels are designed such that the water is never in contact with a vacuum seal. Thus, if a braze joint or weld leaks to vacuum, the water cannot reach the vacuum space.

Two tuners provide better field symmetry, but only one is varied during operations, while the other is held fixed. Vertically, the input coupler (top) and the pump port (bottom) minimize asymmetries in that plane. The calculated angular kick to an off-center beam is  $2.3 \times 10^{-4} \text{ mm}^{-1}$  (horizontal) and  $3.5 \times 10^{-4} \text{ mm}^{-1}$  (vertical).

The last component is a view screen for observing the beam shape after it leaves the gun. Different materials can be used, including BeO, YAG, or CVD diamond. BeO and YAG are best used for low average currents (nanoampere levels), while diamond can withstand microampere average currents. For high bunch charge, short bunch-length beams, it is important to have a smooth surface along the inside of the beam pipe to minimize wakefield effects. Figure 4.35 illustrates how an RF trailer slides into place when the view screen is retracted. The trailer (aluminum), makes RF contact with the beam pipe using spring fingers.

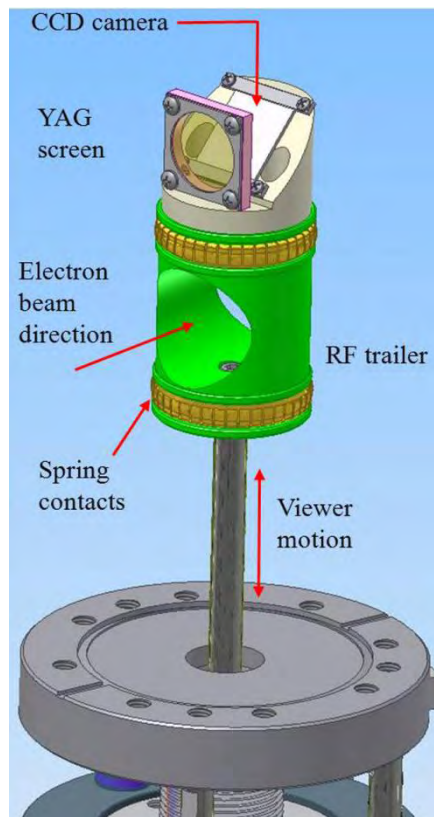


Figure 4.35. A schematic of a retractable view screen mechanism. When the screen is retracted, an RF trailer slides into a cylindrical tube and provides a smooth surface along the beam pipe. The vacuum tube is not shown.

The final subsystem of a DC/SCRF injector is the accelerating module, described in the next section.

#### 4.3.4 Superconducting Acceleration Section

Many authors have detailed the design of superconducting cavities for accelerators (see [4.30] for examples). In this section, I discuss only those aspects related to high average power CW injectors, following the parameter set in Table 4.2.

Accelerating a 100 mA average current CW bunch train to 5 MeV requires 500 kW of RF power. At 1 300 MHz, the highest average power input coupler available operates at 50 kW [4.63]; hence, at minimum, ten input couplers are required. At lower RF frequencies, higher powers can be used as the power per unit area scales as the square of the frequency. Similar to the buncher cavity, having opposing input

feeds helps to symmetrize the fields in the cavity, meaning two couplers per cavity for a total of 5 RF cavities. Figure 4.36 shows an example of a 1 300 MHz input coupler for a superconducting cavity that can operate at 50 kW.

Each RF cavity can have one or more individual, coupled niobium cells. With 5 two-cell cavities, each cavity must provide 1 MV of energy gain, equivalent to a field gradient of  $5 \text{ MV m}^{-1}$ , well within today's capabilities. Figure 4.37 is an example of a two-cell cavity with two opposing ports for the input couplers [4.64], operating between  $5$  and  $15 \text{ MV m}^{-1}$  with a quality factor ( $Q_0$ ) of  $1 \times 10^{10}$ .

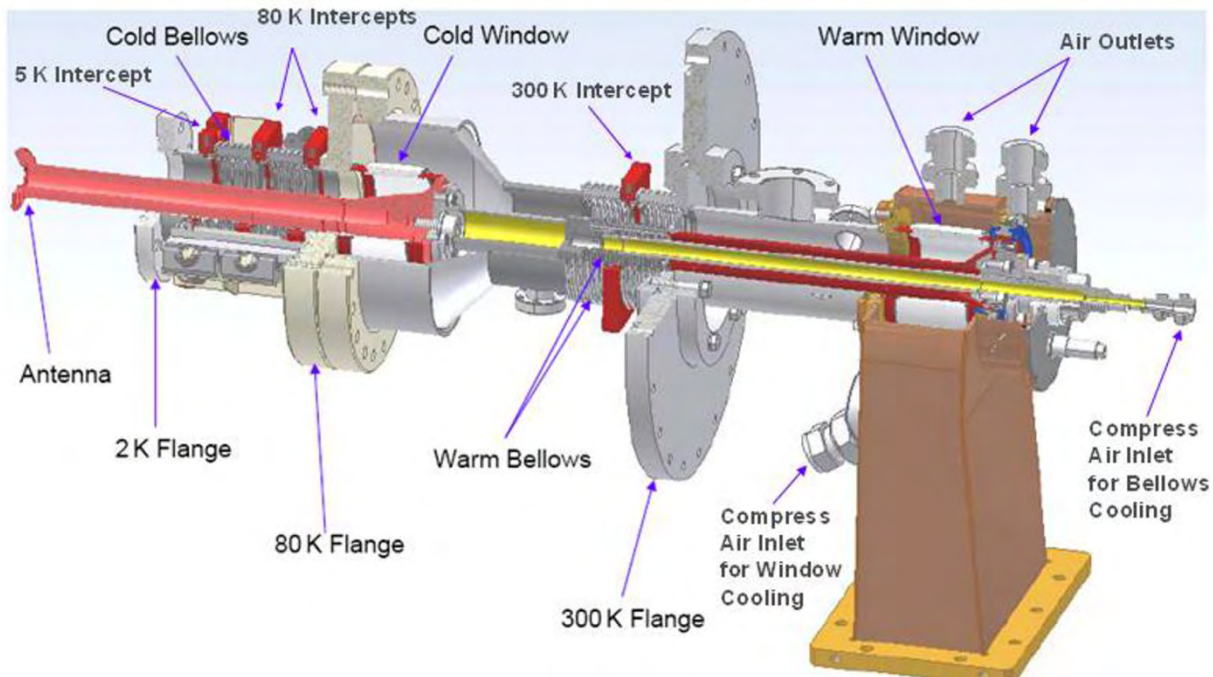


Figure 4.36. A high average power 1 300 MHz input coupler. The top picture shows the actual device, while the bottom cutaway view indicates the inner details and temperature intercepts from warm to cold.

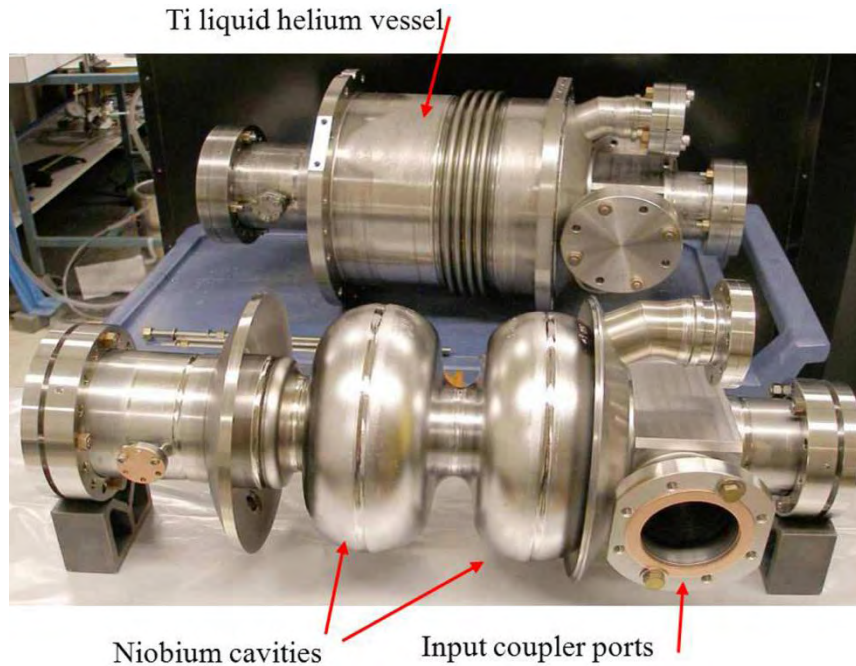


Figure 4.37. The 2-cell niobium cavity with opposing input ports is shown at the bottom. Above, a titanium liquid-helium vessel is welded around the cavity. Its small size limits the amount of liquid helium required.

For lower average power machines, the same cavity can be used for the injector and the main accelerator. At CEBAF, for example, cavities of 5 cells are used. An unintended benefit of having 5 two-cell cavities (opposed to 2 five-cell cavities) is that additional degrees of freedom are available for optimizing the beam properties, *viz.*, 5 gradients and 5 phases. With this configuration, the first and second cavities can be run off-crest to supplement the bunching process, providing an option of increasing the length of the initial bunch to reduce space charge forces. Further, this additional control supports a lower gun voltage, if desired. Beams as low as 200 kV can be straightforwardly captured from the gun by adjusting the phases and gradients of the first few cavities. With a five-cell cavity, the phase slippage due to the non-relativistic beam can decelerate the beam for low gun voltages.



Figure 4.38. An example of an RF HOM inline absorber. The picture at the upper right shows three types of RF absorber tiles mounted on copper heat sinks. The left shows the HOM vacuum vessel with plumbing for cooling gas to remove the heat from the tiles, while the lower right cutaway view shows how the device is assembled.

The last critical component for an accelerating section is a way to absorb the power in the higher order modes (HOM). For the very short bunch lengths envisioned ( $< 1$  mm), the beam can excite resonances at frequencies higher than the fundamental, which can increase beam emittance. There are several options for removing the power from HOMs, using either waveguide dampers, or inline absorbers. Figure 4.38 shows an example of the latter, using various types of absorbing tiles [4.64].

With all of the components in hand, the cavity string can be assembled (Figure 4.39) in a cleanroom to minimize particle contamination, which can compromise the cavity's performance. The string is then inserted into the cryogenic vacuum vessel, where all the input couplers, helium plumbing and instrumentation are attached. Figure 4.40 shows the complete assembly ready to be shipped to its final destination.

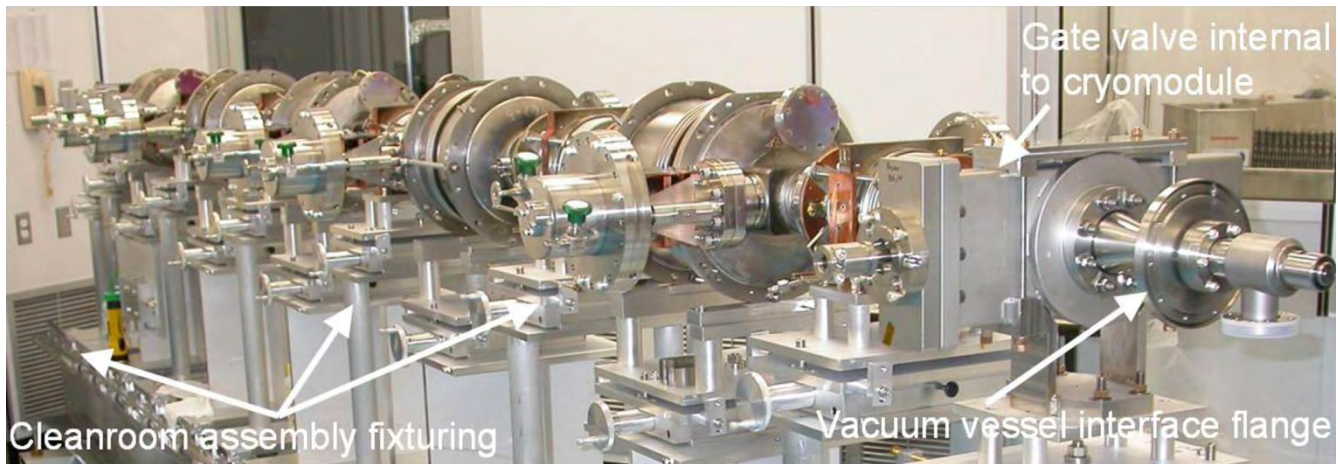


Figure 4.39. An assembled cavity string, consisting of 2 gate valves, 6 HOM absorbers, 5 two-cell cavities. The input couplers are installed after the string is inserted into the cryomodule.



Figure 4.40. The final fully assembled cryomodule ready to ship.

There are other examples of RF designs for ~100 mA average current electron injectors. Figure 4.41 shows a design from Jefferson Laboratory [4.66]. It starts with a 500 kV DC photoemission gun, followed by a solenoid for emittance compensation. The accelerating cavities operate a 748.5 MHz, and at this lower frequency, three single-cell cavities can attain the 5-7 MeV desired beam energy. A third harmonic cavity located between cavities 1 and 2 linearizes energy variations along the bunch.

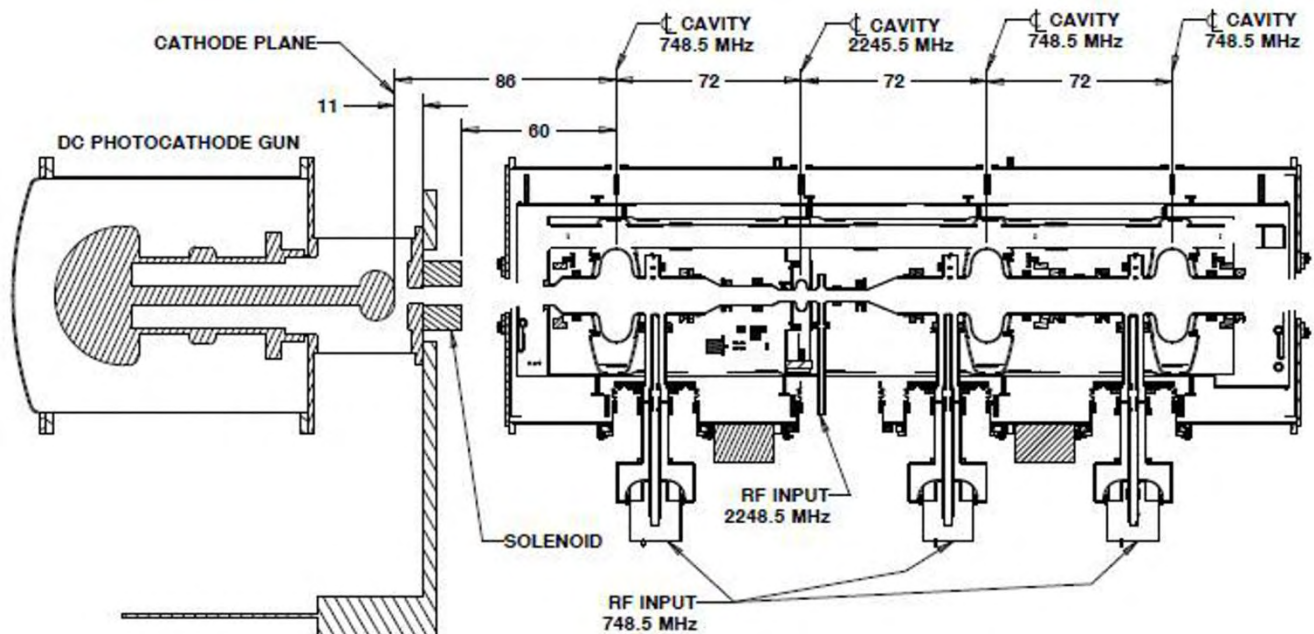


Figure 4.41. Drawing of a Jefferson lab design for a 100 mA injector. [Courtesy of F. Hannon]

## 4.4 SUMMARY

In this chapter, I covered the design and implementation of an electron injector using a high voltage DC photoemission gun and a superconducting RF accelerator. This type of injector is best suited for mid-range bunch charge, high average power applications that require high brightness beams. I described in detail the various sub-systems for a DC/RF injector; many of these parts are well defined. Obtaining ~500 kV operational gun voltages remains difficult, although rapid progress is being made. Cathodes exist with reasonable lifetime for several milliamper beams, but work continues to find low emittance, high efficiency cathodes with long operational lifetime at higher currents. For the RF- and SCRF-systems, tests are underway to prove that the designs are reliable between 10 and 100 mA.

Several groups are working on high average power machines to verify the technologies and to demonstrate the accuracy of the simulations. While DC gun/RF injectors have existed for many decades, the last ten years has seen many advances in gun-, laser-, cathode- and SCRF-technologies that promise to provide a path to reliable, high average power, high brightness electron injectors that can be used in many high performance accelerator applications.

## 4.5 CONFLICT OF INTEREST AND ACKNOWLEDGEMENT

I confirm that this article content has no conflicts of interest and would like to acknowledge the support by the National Science Foundation, grant number DMR-0807731.

**References**

- [4.1] C. K. Sinclair, E. L. Garwin, R. H. Miller *et al.*, "A high intensity polarized electron source for the Stanford Linear Accelerator," in *Proc. AIP Conf.*, vol. 35, 1976, pp. 424-431.
- [4.2] M. B. James and R. H. Miller, "A high current injector for the proposed SLAC linear collider," *IEEE Trans. Nucl. Sci.*, vol. 28, pp. 3461-3463, June 1981.
- [4.3] C. K. Sinclair, "The SLAC lasertron project," in *Proc. AIP Conf.*, vol. 156, 1987, pp. 298-312.
- [4.4] C. K. Sinclair, "A 500 kV photoemission electron gun for the CEBAF FEL," *Nucl. Instrum. Meth. A*, vol. 318, pp. 410-414, July 1992.
- [4.5] R. Alley, H. Aoyagi, J. Clendenin *et al.*, "The Stanford linear accelerator polarized electron source," *Nucl. Instrum. Meth. A*, vol. 365, pp. 1-27, November 1995.
- [4.6] C. K. Sinclair, "DC photoemission electron guns as ERL sources," *Nucl. Instrum. Meth. A*, vol. 557, pp. 69-74, February 2006.
- [4.7] J. Haimson, B. Mecklenburg, G. Stowell *et al.*, "A fully demountable 550 kV electron gun for low emittance beam experiments with a 17 GHz linac," in *Proc. 1997 Particle Accelerator Conf.*, 1997, pp. 2808-2810.
- [4.8] I. V. Bazarov and C. K. Sinclair, "Multivariate optimization of a high brightness DC gun photoinjector," *Phys. Rev. ST Accel. Beams*, vol. 8, pp. 034202-1–034202-14, March 2005.
- [4.9] B. M. Dunham, L. S. Cardman and C. K. Sinclair, "Emittance measurements for the Illinois/CEBAF polarized electron source," in *Proc. 1995 Particle Accelerator Conf.*, 1995, pp. 1030-1032.
- [4.10] D. Dowell, S. Z. Bethel and K. D. Friddell, "Results from the average power laser experiment photocathode injector text," *Nucl. Instrum. Meth. A*, vol. 356, pp. 167-176, March 1995.
- [4.11] I. V. Bazarov, B. M. Dunham and C. K. Sinclair, "Maximum achievable beam brightness from photoinjectors," *Phys. Rev. Lett.*, vol. 102, pp. 104801-1–104801-4, March 2009.
- [4.12] B. E. Carlsten, "New photoelectric injector design for the Los Alamos National Laboratory XUV FEL accelerator," *Nucl. Instrum. Meth. A*, vol. 285, pp. 313-319, December 1989.
- [4.13] I. V. Bazarov, B. M. Dunham, Y. Li *et al.*, "Thermal emittance and response time measurements of negative electron affinity photocathodes," *J. Appl. Physics*, vol. 103, pp. 054901-1–054901-8, March 2008.
- [4.14] K. Smolenski, I. Bazarov, H. Li *et al.*, "Design and Performance of the Cornell ERL dc photoemission gun," in *Proc. AIP Conf.*, vol. 1149, 2008, pp. 1077-1083.
- [4.15] S. H. Kong, D. C. Nguyen, R. L. Sheffield *et al.*, "Fabrication and characterization of cesium telluride photocathodes: A promising electron source for the Los Alamos Advanced FEL," *Nucl. Instrum. Meth. A*, vol. 358, pp. 276-279, April 1995.
- [4.16] I. Bazarov, B. M. Dunham, X. Li *et al.*, "Thermal emittance and response time measurements of a GaN photocathode," *J. Appl. Physics*, vol. 105, pp. 083715-1–083715-4, April 2009.
- [4.17] P. Hartmann, J. Bermuth, D. v. Harrach *et al.*, "A diffusion model for picosecond electron bunches from negative electron affinity GaAs photocathodes," *J. Appl. Physics*, vol. 86, pp. 2245-2249, August 1999.
- [4.18] S. Pastuszka, D. Kratzmann, D. Schwalm *et al.*, "Transverse energy spread of photoelectrons emitted from GaAs photocathodes with negative electron affinity," *Appl. Physics Lett.*, vol. 71, pp. 2967-2969, September 1997.
- [4.19] C. K. Sinclair, P. A. Adderley, B. M. Dunham *et al.*, "Development of a high average current polarized electron source with long cathode operational lifetime," *Phys. Rev. ST Accel. Beams*, vol. 10, pp. 023501-1–023521-21, February 2007.
- [4.20] J. Grames, M. Poelker, P. Adderley *et al.*, "Measurements of photocathode operational lifetime at beam currents up to 10 mA using an improved DC high voltage GaAs photogun," in *Proc. AIP Conf.*, vol. 915, 2007, pp. 1037-1044.

- [4.21] C. K. Sinclair, "High voltage DC photoemission electron guns – current status and technical challenges," *Int. Committee Future Accel. Beam Dynamics Newslett.*, no. 46, August 2008, pp. 97-118.
- [4.22] B. M. Dunham, P. Hartmann, R. Kazimi *et al.*, "Advances in DC photocathode electron guns," in *Proc. AIP Conf.*, vol. 472, 1998, pp. 813-822.
- [4.23] D. H. Dowell, I. Bazarov, B. Dunham *et al.*, "Cathode R&D for future light sources," *Nucl. Instrum. Meth. A*, vol. 622, pp. 685-697, October 2010.
- [4.24] N. Nishimori, I. Bazarov, B. Dunham *et al.*, "DC gun technological challenges," in *Proc. Energy Recovery Linac Workshop*, 2009.
- [4.25] R. E. Kirby, G. J. Collet and K. Skarpass, "An in-situ photocathode loading system for the SLC polarized electron gun," in *Proc. 1993 Particle Accelerator Conf.*, 1993, pp. 3030-3032.
- [4.26] Z. Yu, S. L. Buczowski, N. C. Giles *et al.*, "Defect reduction in ZnSe grown by molecular beam epitaxy on GaAs substrates cleaned using atomic hydrogen," *Appl. Physics Lett.*, vol. 69, pp. 82-84, April 1996.
- [4.27] C. D. Park, S. M. Chung, X. Liu *et al.*, "Reduction in hydrogen outgassing from stainless steels by a medium-temperature heat treatment," *J. Vacuum Sci. Tech. A*, vol. 26, pp. 1166-1171, August 2008.
- [4.28] H. Kurisu, G. Kimoto, H. Fujii *et al.*, "Outgassing properties of chemically polished titanium materials," *J. Vacuum Soc. Japan*, vol. 49, pp. 254-258, February 2006.
- [4.29] F. Rosebury, *Handbook of Electron Tube and Vacuum Techniques*, Woodbury: American Institute of Physics, 1993.
- [4.30] H. Padamsee, *RF Superconductivity: Science, Technology and Application*, Weinheim: Wiley-VCH Verlag, 2009.
- [4.31] Zachary Conway, personal communication, January 2010.
- [4.32] Applied Surface Technologies, Inc., manufactures CO<sub>2</sub> snow guns.
- [4.33] M. Böhnert, D. Hoppe, L. Lilje *et al.*, "Particle free pump down and venting of UHV vacuum systems," in *Proc. 2009 Superconducting RF Conf.*, 2009, pp. 883-886.
- [4.34] SAES Getters, Inc., Viale Italia, 77, 20020 Lainate MI, Italy. Online: <http://www.saesgetters.com/>.
- [4.35] M. L. Stutzman, P. Adderley, J. Brittan *et al.*, "Characterization of the CEBAF 100 kV GaAs photoelectron gun vacuum system," *Nucl. Instrum. Meth. A*, vol. 574, pp. 213-220, January 2007.
- [4.36] D. J. Holder, "First results from the ERL prototype (ALICE) at Daresbury," in *Proc. 2008 Linear Accelerator Conf.*, 2008, pp. 694-698.
- [4.37] P. A. Adderley, J. Clark, J. Grames *et al.*, "Load-locked DC high voltage GaAs photogun with an inverted-geometry ceramic insulator," *Phys. Rev. ST Accel. Beams*, vol. 13, pp. 010101-1–010101-7, January 2010.
- [4.38] P. G. Slade, *The Vacuum Interrupter: Theory, Design and Application*, Raton: CRC Press, Boca, 2008.
- [4.39] R. Latham, Ed., *High Voltage Vacuum Insulation: Basic Concepts and Technological Practice*, London: Academic Press, 1995.
- [4.40] P. Spolaore, G. Bisoffi, F. Cervellera *et al.*, "The large gap case for high voltage insulation in vacuum," in *17<sup>th</sup> Int. Symp. Discharges Elect. Insulation Vacuum*, 1996, pp. 523-526.
- [4.41] F. Furuta, T. Nakanishi, S. Okumi *et al.*, "Reduction of field emission dark current for high-field gradient electron gun by using a molybdenum cathode and titanium anode," *Nucl. Instrum. Meth. A*, vol. 538, pp. 33-44, February 2005.
- [4.42] I. Smith, "The early history of western pulsed power," *IEEE Trans. Plasma Sci.*, vol. 34, pp. 1585-1609, October 2006.
- [4.43] J. Haimson, "Recent advances in high voltage electron beam injectors," *IEEE Trans. Nucl. Sci.*, Vol. 22, pp. 1354-1357, June 1975.

- [4.44] Dielectric Science, Inc., 88 Turnpike Road, Chelmsford, MA, 01824. Online: <http://www.dielectricsciences.com/>.
- [4.45] Claymount Corporation, Anholtseweg 44, De Rietstap, 7091 HB Dinxperlo, The Netherlands. Online: <http://www.claymount.com>
- [4.46] N. H. Malik, A. A. Al-Arainy and M. I. Qureshi, *Elect. Insulation Power Syst.*, New York: Marcel Dekker, Inc, 1997.
- [4.47] J. J. Shea, "Punchthrough of ceramic insulators," in *Proc. IEEE Conf. Electronics Insulation Dielectric Phenomena*, 1990, pp. 441-450.
- [4.48] J. Vines and P. A. Einstein, "Heating effect of an electron beam impinging on a solid surface, allowing for penetration," in *Proc. IEE*, vol. 111, 1964, pp. 921-930.
- [4.49] B. M. Dunham and K. Smolenski, in *Proc. IEEE Int. Power Modulator High Voltage Conf.*, 2010, pp. 92-101.
- [4.50] F. Liu, I. Brown, L. Phillips *et al.*, "A method of producing very high resistivity surface conduction on ceramic accelerator components using metal ion implantation," in *Proc. 1997 Particle Accelerator Conf.*, 1997, pp. 3572-3574.
- [4.51] R. Nagai, R. Hajima, N. Nishimora *et al.*, "High-voltage testing of a 500-kV DC photocathode electron gun," *Rev. Sci. Instrum.*, vol. 81, pp. 033304-1–033304-5, February 2010.
- [4.52] S. V. Benson, G. Biallas, D. Bullard *et al.*, "An inverted ceramic DC electron gun for the Jefferson Laboratory FEL," in *Proc. Free Electron Laser Conf.*, 2009, pp. 383-385.
- [4.53] J. D. Cockcroft and E. T. Walton, "Experiments with high velocity positive ions. II. The disintegration of elements by high velocity protons," in *Proc. Royal Society London A*, 1932, pp. 229-242.
- [4.54] C. Hernandez-Garcia, T. Siggins, S. Benson *et al.*, "A high average current DC GAAS photocathode gun for ERLS and FELS," in *Proc. 2005 Particle Accelerator Conf.*, 2005, pp. 3117-3119.
- [4.55] R. J. van de Graaff, "High voltage electromagnetic apparatus having an insulating magnetic core," U.S. Patent No. 3,187,208, June 1, 1965.
- [4.56] U. Uhmeyer, "KSI's cross insulated core transformer technology," in *Proc. AIP Conf.*, vol. 1149, 2009, pp. 1099-1103.
- [4.57] M. E. Cunco, "The effects of electrode cleaning and conditioning on the performance of high-energy, pulsed-power devices," in *18<sup>th</sup> Int. Symp. Discharges Elect. Insulation Vacuum*, 1998, pp. 721-730.
- [4.58] S. Bajic and R. V. Latham, "A new perspective on the gas conditioning of high-voltage vacuum-insulated electrodes," *J. Physics D: Appl. Physics*, vol. 21, pp. 943-950, 1988.
- [4.59] J. Hao, F. Zhu, S. Quan *et al.*, "3.5-cell superconducting cavity for DC-SRF photoinjector at Peaking University," in *Proc. 2009 Superconducting RF Workshop*, 2009, pp. 205-207.
- [4.60] D. H. Dowell, E. Jongewaard, J. Lewandowski *et al.*, "The development of the linac coherent light source RF gun," *Int. Committee Future Accel. Beam Dynamics Newslett.*, no. 46, August 2008, pp. 162-192.
- [4.61] A. Chao and M. Tigner, Eds., *Handbook of Accelerator Physics and Engineering*, Singapore: World Scientific Press, 1999, pp. 102.
- [4.62] V. Veshcherevich and S. A. Belomestnykh, "Buncher cavity for ERL," in *Proc. 2003 Particle Accelerator Conf.*, 2003, pp. 1198-1200.
- [4.63] V. Veshcherevich, I. Bazarov, S. Belomestnykh *et al.*, "Input coupler for ERL injector cavities," in *Proc. 2003 Particle Accelerator Conf.*, 2003, pp. 1201-1203.
- [4.64] V. Shemelin, S. Belomestnykh, R. L. Geng *et al.*, "Dipole-mode-free and kick-free 2-cell cavity for the SC ERL injector," in *Proc. 2003 Particle Accelerator Conf.*, 2003, pp. 2059-2061.

An Engineering Guide to Photoinjectors, T. Rao and D. H. Dowell, Eds.

- [4.65] V. Shemelin, P. Barnes, B. Gillet *et al.*, “Status of HOM load for the Cornell ERL injector,” in *Proc. 2006 European Particle Accelerator Conf.*, 2006, pp. 478-480.
- [4.66] F. E. Hannon and C. Hernandez-Garcia, “Simulation and optimization of a 100 mA DC photo-injector,” in *Proc. 2006 European Particle Accelerator Conf.*, 2006, pp. 3550-3552.